

SELECTIVE REMOVAL OF DUAL DYES FROM AQUEOUS SOLUTIONS
USING METAL ORGANIC FRAMEWORK (MIL-53(AI))

by

Miral Osama Yacoub Al Sharabati

A Thesis presented to the Faculty of the
American University of Sharjah
College of Engineering
In Partial Fulfillment
of the Requirements
for the Degree of

Master of Science in
Chemical Engineering

Sharjah, United Arab Emirates

November 2019

Approval Signatures

We, the undersigned, approve the master's Thesis of Miral Osama Yacoub Al Sharabati

Thesis Title: Selective Removal of Dual Dyes from Aqueous Solutions Using Metal Organic Framework (MIL-53(Al))

Signature

Date of Signature
(dd/mm/yyyy)

Dr. Rana Sabouni
Assistant Professor, Department of Chemical Engineering
Thesis Advisor

Dr. Yassir T. Makkawi
Associate Professor, Department of Chemical Engineering
Thesis Committee Member

Dr. Mehdi Ghommem
Assistant Professor, Department of Mechanical Engineering
Thesis Committee Member

Dr. Sameer Al- Asheh
Interim Head, Department of Chemical Engineering

Dr. Lotfi Romdhane
Associate Dean for Graduate affairs and Research, College of Engineering

Dr. Naif Darwish
Acting Dean, College of Engineering

Dr. Mohamed El-Tarhuni
Vice Provost for Graduate Studies

Acknowledgement

I would like to thank my thesis advisor Dr. Rana Sabouni for her continuous support, professional guidance, and valuable comments and engagement throughout the entire process of this thesis. As my advisor and mentor, she has provided me with a great deal of knowledge and steered me in the right direction whenever I had any doubts or questions. This work would not have been possible without her help and dedication.

Furthermore, I would like to thank my fellow lab mate Mr. Abdollah Karami for familiarizing me with the topic, continuously supporting me and providing valuable suggestions that were helpful in performing the experiments.

I would like to thank Mr. Ibrar Samad and Ms. Marah Ali for their moral support and continuous encouragement throughout the whole process.

Special thanks to the American University of Sharjah and the Chemical Engineering Department for granting me the Graduate Teaching Assistantship and funding this research.

I would also like to thank my thesis committee members, Dr. Yassir T. Makkawi and Dr. Mehdi Ghommem for their valuable comments and remarks that helped me pave the way for completing this work.

Finally, I would like to express my sincere gratitude to my parents and siblings for their love, guidance, and continuous support throughout my studies and the process of completing this thesis.

Dedication

To my family...

Abstract

Organic dyes released from many industries such as textile, leather, and paper industries can be a threat to the environment and living creatures. Adsorption stands out as one of the favorite dye removal methods among the countless tried-and-tested techniques due to its excelling capability to remove nearly any kind of dyes. In the last two decades, there has been an ongoing research on Metal Organic Frameworks (MOFs) for the removal of dyes from wastewater owing to their extraordinary properties, high adsorption capacities, high stability and regenerability. In this thesis, the adsorption process of the cationic dye Malachite Green (MG) and the anionic dye Methyl Orange (MO) onto a MOF, namely, MIL-53(Al) was studied under several experimental parameters. Batch experiments were performed to investigate the feasibility of this MOF as possible adsorbent for the removal of MG and MO from both single and binary-dye aqueous solutions. Experimental results revealed that MIL-53(Al) can quickly bind to both types of dyes with high removal efficiency of more than 95%. The effects of different parameters such as adsorbent dosage, initial concentration of dye solution, pH of the solution, and temperature on the adsorption process were examined. Adsorption kinetic data were then fitted using pseudo first-order, pseudo second-order, elovich, and intraparticle diffusion models, showing that pseudo second-order model had the best fit for both dyes among the other models in both single and binary-dye systems with $R^2 > 0.996$. Moreover, adsorption isotherm models of Langmuir and Freundlich were studied and the isotherm data was found to be in good agreement with the Freundlich isotherm for both dyes. Thermodynamics studies of change in Gibbs free energy, enthalpy, and entropy were carried out and showed that the adsorption of both dyes was endothermic and spontaneous. The selectivity test for an equimolar binary-dye solution containing both MG and MO suggested the higher affinity of MIL-53(Al) towards MO over MG, as it reached a value of 13.582 at the optimum conditions. Finally, excellent reusability of MIL-53(Al) was shown by utilizing it for 4 cycles of adsorption-desorption with almost no reduction in the adsorption capacity, bringing about additional examination of its applicability.

Keywords: *Wastewater treatment, Adsorption, Metal Organic Frameworks (MOFs), MIL-53(Al), Malachite green, Methyl orange.*

Table of Contents

| | |
|---|----|
| Abstract..... | 6 |
| List of Figures..... | 9 |
| List of Tables..... | 11 |
| List of Abbreviations..... | 12 |
| Chapter 1. Introduction..... | 13 |
| 1.1. Overview..... | 13 |
| 1.2. Thesis Objectives..... | 16 |
| 1.3. Research Contribution..... | 16 |
| 1.4. Thesis Organization..... | 17 |
| Chapter 2. Background and Literature Review..... | 18 |
| 2.1. Dyes..... | 18 |
| 2.2. Types of Dyes..... | 18 |
| 2.2.1. Malachite green and methyl orange as examples of dyes..... | 19 |
| 2.3. Dye Removal Methods..... | 20 |
| 2.3.1. Biological treatment methods..... | 21 |
| 2.3.2. Chemical treatment methods..... | 23 |
| 2.3.3. Physical treatment methods..... | 25 |
| Chapter 3. Experimental Work and Methodology..... | 37 |
| 3.1. Materials..... | 37 |
| 3.2. Adsorption Experiments..... | 37 |
| 3.3. Characterization..... | 40 |
| 3.4. Adsorption Kinetics..... | 40 |
| 3.5. Adsorption Isotherms..... | 42 |
| 3.6. Adsorption Thermodynamics..... | 43 |
| 3.7. Selectivity of Binary-Dye Adsorption..... | 43 |
| 3.8. Factorial Design..... | 44 |
| Chapter 4. Results and Analysis..... | 45 |
| 4.1. Characterization Tests..... | 45 |
| 4.2. Removal Efficiencies..... | 47 |
| 4.3. Point of Zero Charge and Effect of pH..... | 48 |
| 4.4. Effect of Initial Concentration..... | 50 |
| 4.5. Effect of Amount of MOF..... | 51 |

| | |
|--|----|
| 4.6. Adsorption Kinetics..... | 52 |
| 4.7. Adsorption Isotherms | 56 |
| 4.8. Adsorption Thermodynamics | 57 |
| 4.9. Selectivity of Binary-Dye Adsorption..... | 59 |
| 4.10. Regeneration of MIL-53(Al)..... | 60 |
| 4.11. Factorial Design | 60 |
| Chapter 5. Conclusions and Future Work..... | 69 |
| References..... | 71 |
| Vita..... | 79 |

List of Figures

| | |
|--|----|
| Figure 1: Classification of dyes based on solubility [15]. | 19 |
| Figure 2: Zeolite structure [46]. | 31 |
| Figure 3: Chemical structure of a classic MOF, MOF-5 [53]. | 32 |
| Figure 4: Organic linkers used for MOF synthesis [52]. | 33 |
| Figure 5: Calibration curve for MG solution. | 39 |
| Figure 6: Calibration curve for MO solution. | 39 |
| Figure 7: XRD patterns of MIL-53(Al) before and after MO and MG adsorption. Pattern from literature reported by Li et al. [70]. | 46 |
| Figure 8: FT-IR spectra of MIL-53(Al) before and after MO and MG adsorption. | 47 |
| Figure 9: Comparison of (a) MO removal efficiency and (b) MG removal efficiency onto MIL-53(Al) in single and binary-dye solutions. | 48 |
| Figure 10: (a) Effect of solution pH on the adsorbed amount of MO and MG over MIL-53(Al); (b) Determination of MIL-53(Al) point of zero charge by plotting ΔpH vs. initial pH. | 49 |
| Figure 11 : Effect of initial concentration on the adsorbed amount of MG in (a) single-dye solution and (b) binary-dye solution. | 50 |
| Figure 12: Effect of initial concentration on the adsorbed amount of MO in (a) single dye solution and (b) binary-dye solution. | 50 |
| Figure 13 : Effect of MIL-53(Al) dosage on the adsorbed amount of MG in (a) single dye solution and (b) binary-dye solution at an initial concentration of 13 mg/L. | 51 |
| Figure 14: Effect of MIL-53(Al) dosage on the adsorbed amount of MO in (a) single dye solution and (b) binary-dye solution at an initial concentration of 13 mg/L. | 52 |
| Figure 15: PSO models for the removal of (a) MG and (b) MO in single and binary solutions at an initial concentration of 13 mg/L and 50 mg of MOF. | 55 |
| Figure 16: Intraparticle Diffusion model for the removal of (a) MG and (b) MO in single and binary solutions with 50 mg of MOF. | 55 |
| Figure 17: Freundlich model for the removal of (a) MG and (b) MO in single dye solutions with 10 mg of MOF at 298 K. | 56 |
| Figure 18: Van't Hoff plot for ΔH° and ΔS° measurement of MO and MG adsorption on MIL-53(Al). | 58 |

| | |
|---|----|
| Figure 19: Adsorption selectivity for binary-dye solutions at initial concentrations of 7 and 13 mg. L ⁻¹ with addition of (a) 10 and (b) 50 mg of MIL-53(Al)..... | 59 |
| Figure 20: Effect of number of cycles of MIL-53(Al) on MG and MO binary adsorption at 298 K, C _o = 13 mg/L, and m=50 mg. | 60 |
| Figure 21: Cube plot for adsorption capacity of (a) MO and (b) MG removal. | 62 |
| Figure 22: Main effects plot for adsorption capacity of (a) MO and (b) MG removal. | 64 |
| Figure 23: Interaction effects plot for adsorption capacity of (a) MO and (b) MG..... | 66 |
| Figure 24: Pareto chart of the effects of (a) MO and (b) MG removal..... | 67 |

List of Tables

| | |
|--|----|
| Table 1: Chemical Properties of MG and MO [18], [19]. | 20 |
| Table 2: International standard of dye wastewater discharge into the environment [3] | 21 |
| Table 3: Advantages and disadvantages of different biological dye removal methods [25], [26] | 22 |
| Table 4: Comparison between chemical and physical carbon activation processes [3] | 29 |
| Table 5: Adsorption capacity and surface areas for different types of activated carbon [3] | 30 |
| Table 6: Malachite Green and Methyl Orange adsorption capacities with various MOFs | 36 |
| Table 7: Kinetic parameters for MO adsorption in single and binary-dye solutions | 53 |
| Table 8: Kinetic parameters for MG adsorption in single and binary solutions | 54 |
| Table 9: Adsorption isotherm parameters of single dye adsorption by MIL-53(Al) at various temperatures | 57 |
| Table 10 : Thermodynamic parameters of MO and MG adsorption by MIL-53(Al) | 58 |
| Table 11: Selectivity at different initial concentrations and MOF dosage | 59 |
| Table 12: The factorial design's factors and levels | 61 |
| Table 13: Design matrix and results for MG and MO adsorption capacity | 61 |
| Table 14: Estimated effects and coefficients for adsorption capacity of MIL-53(Al) for both dyes | 63 |

List of Abbreviations

| | |
|-------|---|
| FT-IR | Fourier Transform Infrared spectroscopy |
| MG | Malachite Green |
| MO | Methyl Orange |
| MOF | Metal Organic Framework |
| XRD | X-Ray Powder Diffraction |

Chapter 1. Introduction

1.1. Overview

Environmental pollution has reached a disturbing level that is increasingly threatening the environment. This is due to the fast urbanization and the constantly growing world population not to mention the fast industrialization which generates wide quantities of dangerous wastes and lethal gases besides the required products. Critical water pollution happens when industrial outflow produces risky wastewaters that are emitted into the environment without being treated. It has been discovered that different pollutants like pharmaceutical and personal care products (PPCPs), dyes, herbicides/pesticides, spilled oil, persistent organic pollutants (POPs), and heavy metal ions are present in the various water resources [1].

Organic dyes released from many industries can be a threat to the environment and living creatures. Textile, leather, and paper industries are some of the important industries that require the utilization of synthetic dyes due to their color giving characteristics. It is reported that 700 000 tonnes of different coloring from around 100 000 attainable dyes are produced annually. The majority of dyes are discharged without additional care into the aquatic environment as soon as their objective is fulfilled. The textile industry is declared to use and produce the largest amount of dyestuff and dye wastewater at roughly 10 000 tonnes and 100 tonnes each year, respectively [1], [2]. The massive water demand and the high utilization of pigmentation in the processes of this industry produce great amounts of dye wastewater. Such processes include dyeing, bleaching, wet finishing, scouring...etc. As soon as the process is finished, the mixture remaining from the preparation of certain blends of pigmentation, chemicals and water is discarded into the environment. The failure of the dye mixture, that is the dye chemicals and molecules, to be fully attached on to a textile or cloth results in the existence of dye effluents remaining from the textile industry. Plenty of dangerous chemicals are present in the dye wastewater, which can jeopardize the humans and animals' lives since they are naturally toxic. Some of these chemicals include acetic acid, soap, softener, caustic soda...etc. [3].

The self-purification and the oxygen transfer techniques of water reservoirs will become disrupted when acidic dye effluents at high temperatures are discharged instantly following dyeing processes. The ecosystem will be threatened by these effluents which will pollute the water bodies making them unfit for utilization. Since they have a lower density of 0.8 kg/m^3 than that of water, 1.0 kg/m^3 , dye effluents will create a visual layer on top of the water surface causing an increase in water turbidity. This prevents the permeation of sunlight needed by water living beings for photosynthesis and respiration kind of processes ending their lifetime. Contact with dye effluents can result in skin irritation; that is eye burns or everlasting eye damage. Inhalation of the chemicals existing in the dyes that are disposed into water after evaporation can cause breathing difficulties. Ingestion of dyes can result in nausea and mouth burns. So, wastewater must be treated from dye effluents to cease their harmful effects on the living things [3].

Wastewater treatment processes play a huge part in the society well-being and environment as they are designed to clean off wastewater from the existing pollutants to be safely reused or removed. After being treated, wastewater can be either reclaimed or safely removed. If recycled, it will be considered as non-potable water that can be used for many purposes such as landscape and crop irrigation, laundry, car washing and in many other industries [4]. While if removed, no severe outcomes shall result from sending it back into the environment. It is always favorable for the treated wastewater to be reclaimed and reused instead of giving it off, as this would be of great benefit to both the environment and the industry. For instance, countries with water shortage consider it an absolute necessity to recycle the treated wastewater since it would retain resources and grant essential financial profits, for the recycling processes cost much less than the seawater desalination processes. There are different processes involved in the municipal sewage water treatment. These include pre-treatment, primary, secondary and tertiary treatment.

Pre-treatment includes the screening and disposal of big matters such as leaves, sanitary substances, sticks, diapers, etc. from the sewage. This is because the process bacteria can not readily decompose them and may result in the equipment being plugged or destroyed. Then, these objects are either directed to landfill sites or

burnt after being dried Sewage is then directed into a grit chamber for the settlement of the sand, gravel and grit to the base.

Primary treatment stage takes place after the completion of screening and removal of grit since sewage will still include suspended solids together with organic and inorganic materials. Sewage will be streamed to bigger tanks called sedimentation tanks. The sludge will be settled in the sedimentation tank when the speed of the flow is decreased. Then by pumping, it will be removed from the tanks and can then be treated to be utilized as a fertilizer or discharged. The fats and oil will come to the surface and create a foam that will be settled down and partly digested by aerobic bacteria or else can be retrieved for saponification. This stage alone does not meet the requirements for better water quality; therefore, a secondary treatment stage is needed [5].

The liquid between the sludge and the foam is processed in the secondary treatment stage. Seed sludge is added for additional break down of the waste water [6]. In this step, oxygen is introduced by pumping air to the sewage in large aeration tanks in which aerobic bacteria and other microorganisms grow and are used to crack the organic materials existing in the liquid segment of the sewage [6], [7]. Moreover, they minimize the quantity of other contaminants, detergents, etc. and the produced liquid is normally considered safe for release to a waterbody except if the waterbody is already contaminated. This process lasts for a duration of 3-6 hours.

Tertiary treatment is the third stage of wastewater treatment. If the secondary treatment produces an effluent that is not completely clean for release, advanced treatment will be called for by the Environment Agency to have cleaner water. The reason behind the water not being clean might be due to the sensitivity of the stream it is released into, or it may have uncommon plants and animals, or because it is already contaminated by a septic tank. Phosphorous or Ammoniacal Nitrogen is what needs to be minimized in the tertiary treatment. If there was phosphorous present, then it must be removed by an ongoing dosing process. Nitrifying and then de-nitrification process will be needed if Ammoniacal Nitrogen is the issue, for it converts it to Nitrogen gas that is harmless to the environment. Lastly, a tanker will take off the sludge frequently for additional processing by aerobic or anerobic operations and then have it discarded

or recycled. After being treated, the water can be utilized for irrigation, released into a water body or utilized for deep drainage or agriculture if it is clean enough [8].

This system was carried out for dye wastewater treatment for some time till it was ceased because of high price of operation and maintenance as well as the limitation posed by such methods [3]. Presently, there is an ongoing research on the ideal dye removal technique in order to reuse and reclaim dye wastewater.

1.2. Thesis Objectives

The primary objective of this paper is to examine a type of Metal Organic Frameworks (MOFs), namely, MIL-53(Al) as a potential adsorbent for the removal of cationic and anionic dyes from wastewater. Adsorption process is the method to be used to treat the wastewater that contains dyes, as both single and binary-dye solutions were investigated. The effect of different factors such as adsorbent dosage, initial concentration of dye solution, pH of the solution, temperature, and contact time on the adsorption capacity were examined in batch experiments. The experimental data were fitted to multiple kinetic and isotherm models and the thermodynamic parameters were computed. The selectivity of an equimolar MG/MO solution was calculated to determine which dye had a higher selective adsorption over the other. Evaluation of the regenerability of MIL-53(Al) was performed over several cycles. Full factorial design was developed to examine the main effects and their interactions on the adsorption capacity of MIL-53(Al) in a MG/MO solution.

1.3. Research Contribution

The contributions of this thesis can be briefed as follows:

- Propose Metal Organic Frameworks (MOFs) as promising adsorbents for the removal of anionic and cationic dyes from aqueous solutions.
- Propose adsorption kinetics, isotherms and thermodynamics that best fit the experimental data to evaluate the adsorption performance.
- Propose MIL-53(Al) for selective adsorption of dyes from binary-dye solutions.
- Study reusability of MIL-53(Al) for practical application.

1.4. Thesis Organization

The rest of the chapters of the thesis are organized as follows: Chapter 2 provides background about the different types of dyes and their classification along with the different methods that are used for the treatment of dye-containing wastewater. Chapter 3 describes the materials and the methodology employed in this work. A discussion of the results obtained from this study is presented in Chapter 4. Lastly, Chapter 5 provides a conclusion to this thesis and some recommendations for future work.

Chapter 2. Background and Literature Review

2.1. Dyes

Dyes are colorful materials created to provide substances like papers, textiles or any colorable substance a color or shade. This is viable since dyes have the ability to being attached onto any adjustable matter [9], [10]. Humans have been using dyes for more than a thousand years for plenty of practices. By using naturally accessible matter like insects or plants, natural dyes are generated on a small scale. Nevertheless, the pitfalls with such dyes were the lack of diversity in addition to easily growing dim in the case of sunlight exposure or being washed [3], [2]. Since the demand for dyes is increasing, synthetic dyes were lately brought to light and their manufacture in large scales began. William Henry Perkin originated a wide domain of synthetic dyes in 1856 detecting different bright, colorfast shades for plenty of applications [11]. The issue that natural dyes had was settled by this discovery, but novel problems emerged from the discharge of dye wastewater into the environment without being properly treated. Due to the toxicity of dyes by nature, their existence in water bodies threatened living things resulting in serious outcomes [12]. While it appears that continuing to utilize natural dyes is a preferable option, it was noted that it was just as unfavorable as using synthetic dyes solely. This is due to the fact that a mordant, which is a type of binding agent that helps natural dyes to connect to substances, is needed for the natural dyes to get attached to textile [1]. Mordants are more harmful and hazardous than synthetic dyes [11]. Dye molecules consist of two crucial parts: the chromophores, which are accountable for the color generation and the auxochromes, which improve the affinity towards the textile [13]. Dyes are created as complex organic materials to withstand the degradation in case there is water contact, bright illumination or exposure to high heat sources [3].

2.2. Types of Dyes

A lot of kinds of commercial dyes exist out there and they can be categorized by their chemical structure, color and purpose methods [9]. Several dyes are produced in the ultimate form and then put on the textile while others are prepared on the textile itself (Ingrain dyes). They can also be classified by their solubility as shown in Figure 1. The most generated and used type of dyes globally is the azo dyes having a production rate of 65-70% [14]. All commercial dyes are grave by nature no matter

what structure they have. That is why it is undesired for these dyes to get in the environment without being treated. This has raised concerns and induced environmentalists to come up with methods for the constant removal of these dyes from water sources [3].

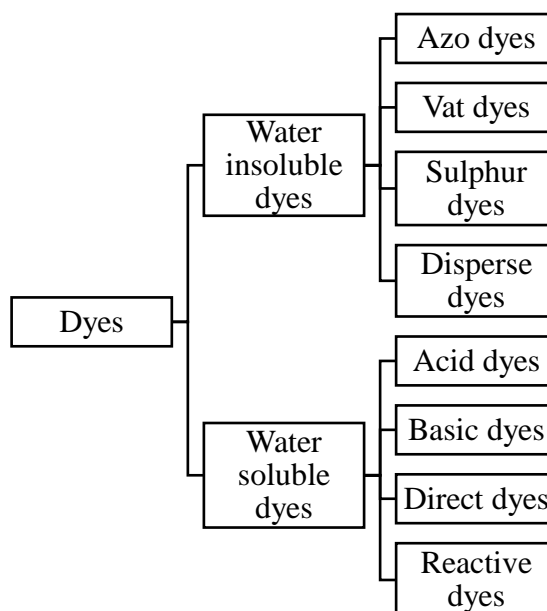


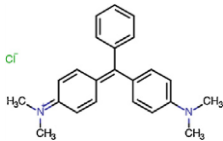
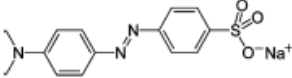
Figure 1: Classification of dyes based on solubility [15].

2.2.1. Malachite green and methyl orange as examples of dyes. In this work, Malachite Green (MG) and Methyl Orange (MO) will be the dye micropollutants that need to be removed from wastewater. Methods of dye removal will be discussed in the following parts of the literature review with an emphasis of particularly MG and MO removal. Malachite Green is a cationic dye classified in the triphenylmethane class, dissolvable in water, and takes the form of crystalline green powder. This dye is widely utilized for the dyeing of silk, cotton, paper and leather products. Since Malachite Green is mutagenic and carcinogenic by nature, it can bring about acute health effects on the kidney, liver and nervous system.

Moreover, a small concentration of MG has the ability to color huge water bodies which results in reducing photosynthesis by blocking light permeation and thus prevents the growth of marine life [16]. Methyl Orange, on the other hand, is an anionic dye that is used in textile, paper, and pharmaceutical industries. It is also used

as a pH indicator in titration, since at a basic pH it generates a yellow color in aqueous solutions, whereas a red color is produced in acidic solutions. It is also considered mutagenic and can result in acute health problems [17]. Therefore, wastewater containing MG and MO should be properly treated to protect the environment and the living things. Table 1 presents the chemical properties and characteristics of Malachite Green and Methyl Orange.

Table 1: Chemical Properties of MG and MO [18], [19].

| Generic Name | Malachite Green | Methyl Orange |
|--------------------------------------|---|---|
| Chemical Formula | $C_{23}H_{25}ClN_2$ | $C_{14}H_{14}N_3NaO_3S$ |
| Molecular Weight ($\frac{g}{mol}$) | 364.911 | 327.33 |
| Type of dye | Cationic | Anionic |
| $\lambda_{max}(nm)$ | 617 | 464 |
| Chemical structure |  |  |

2.3. Dye Removal Methods

Previously, disposal of dye wastewater into the environment was not given careful thought. Light was shed on this problem after health issues began to emerge in the past 30 years [20]. After that, in order to come up with solutions, information on dyes, their utilization, and their removal methods were researched. Plenty of pollutants exist in dye wastewater like dissolved salts (TDS and TSS), chemical oxygen demand (COD), biological oxygen demand (BOD), colors and hazardous chemicals [3]. Table 2 presents the international acceptable standard dye wastewater discharge into the environment. Recently, many researches are being conducted to discover the perfect dye removal technique in order to retrieve and reuse the dye wastewater [21]. Regardless of the existence of a good deal of methods of dye removal from wastewater, all these techniques have ingrained limitations and their own features and drawbacks. The methods can be separated into three classes: biological, chemical and physical treatments [9].

Table 2: International standard of dye wastewater discharge into the environment [3]

| Factor | Standard allowed |
|--------------------------------|------------------------------|
| Suspended Solids (TDS and TSS) | Below 20 mg/L |
| Chemical Oxygen Demand (COD) | Below 50 mg/L |
| Biological Oxygen Demand (BOD) | Below 30 mg/L |
| Color | Below 1 ppm |
| pH | Between 6-9 |
| Temperature | Below 42°C |
| Toxic pollutants | Not allowed to be discharged |

2.3.1. Biological treatment methods. The standard biological technique is the frequently and widely used dye removal technique for dye wastewater treatment in nearly all countries. Depending on the presence or absence of oxygen, the process can be aerobic or anaerobic, respectively [22]. Commonly recognized as the traditional technique, a combination of aerobic and anaerobic process is performed before the discharge of dye wastewater into the environment. In this technique, a prepared sludge is used to crack complex dye particles. This technique was selected as the go-to dye removal technique since it is inexpensive and can be achieved smoothly [23]. In fact, dangerous particles from dye effluent will not be totally ejected by only this treatment, that is why color will still be visible in the water [24]. Even though the treatment of chemical oxygen demand is done by this method, the water will still be toxic and include dyes.

Aside from this technique, there are other biological dye removal techniques available. Adsorption by microbial biomass is one method where dye particles are adsorbed by a mixture of organic living things. Another method is microbial cultures where a mixture of bacteria with chemicals or other bacteria is used to eject dye molecules. Other methods include algae degradation and fungal cultures where algae and fungus, respectively eat up dye molecules for self-growth. The advantages and disadvantages of these mentioned methods are presented in Table 3. Biological

treatment techniques include some sort of living things in their operation. That is why their main drawback is the living organisms' growth rate. Anticipating its growth rate and reactions can be difficult sometimes, so system instability is popular in this kind of dye removal methods [3]. Moreover, some technical limitations of the biological treatment method may include the need of a big land area, sensitivity toward diurnal variation and toxicity of several chemicals, and less pliability in function and design. Furthermore, even though a lot of organic molecules are degraded in the biodegradation processes, some are intractable because of their artificial organic origin and complex molecular structure [20]. Biological dye removal methods have a removal percentage ranging from 76 to 90.1% [3].

Table 3: Advantages and disadvantages of different biological dye removal methods [25], [26]

| Method | Advantages | Disadvantages |
|---------------------------------|--|--|
| Aerobic-anaerobic combination | Completely decolorize a diversity of dye kinds, cheap, no foam generation | Not complete elimination of all dye molecules, generation of methane and hydrogen sulphide as by-products, great land area needed, sludge production, time consuming |
| Adsorption by microbial biomass | Some dyes have extraordinary affinity towards microbial mass | Does not work on all dyes |
| Microbial cultures | Fast decolorization in 30h | Effective to certain dyes, large scale implementation due to high cost |
| Algae degradation | Easily attainable, cheap, environmentally friendly method, dye consumption | System instability |
| Fungal cultures | Instant elimination of different kinds of dyes, flexible process | High growth rate, nitrogen confined area is required for growth, need for large reactors for 100% removal, system instability |

2.3.2. Chemical treatment methods. Chemical treatment techniques use chemistry or its theories to remove dyes. Oxidative processes are the generally applied techniques for decolorization by chemical methods. This is primarily because of its ease of usage. Hydrogen Peroxide (H_2O_2) is normally the major oxidizing agent. This agent requires activation by some measures such as UV light. The method in which the H_2O_2 is activated affects the type of chemical decolorization. Chemical oxidation ejects the dye from the dye wastewater by oxidation, producing aromatic ring cleavage of the dye particles [23]. Chemical treatment means are more expensive than biological and physical treatment techniques except for the electrochemical degradation process which utilizes electro-coagulation or non-soluble anodes to consume dye particles. In addition, chemical treatment techniques are commercially unappealing, need certain apparatus and great electrical energy. The utilization of chemical reagents and cumulation of concentrated sludge contribute to the probability that a secondary pollution issue will come to light [20]. Chemical dye removal processes displayed the highest percentage of dye removal among other methods ranging from 88.8 to 99% [3].

Fenton's reagent. Wastewaters that are reluctant to biological methods or toxic to living organisms can be treated using Fenton's reagent (H_2O_2 – *Fe (II) salts*) [27]. Dissolved dyes are removed from the effluent by utilizing the action of sorption or bonding and this has been proven to be efficient in decolorizing soluble and insoluble dyes [28]. Formation of sludge during the flocculation of the reagent and the dye particles is a considerable drawback of this technique. Burning the sludge is one way to dispose it and generate power at the same time, but this is considered far away from being eco-friendly by some environmentalists. The behavior relies on the production of the ultimate floc and its settling quality even though there is no coagulation with cationic dyes. The generated floc with acid, direct, vat and reactive dyes is of poor quality and bad settlement resulting in moderate outcomes even though these dyes normally coagulate [23].

Ozonation. Ozone was first introduced as an oxidizing agent in the early 1970s. Since it has a higher instability, with an oxidation potential of 2.07, than chlorine (1.36) and H_2O_2 (1.78), it is considered a quite useful oxidizing agent.

Degradation of chlorinated hydrocarbons, phenols, pesticides and aromatic hydrocarbons is possible when oxidized by ozone [29]. Based on the color and remaining COD to be ejected with no sludge or remains development, the portion of ozone to be used on the dye wastewater can be determined. After ozonation, the color will be removed from wastewater and a low amount of COD would be present making it convenient for being released into waterbodies. The volume of effluent and sludge will not grow since ozone can be used in its gaseous phase. Ozonation works best for double-bonded dye particles. It can be utilized together with a physical technique to avoid carcinogenic or poisonous characteristics resulting from the smaller molecules that the chromophore groups may be broken into. The short half-life of ozonation is a major drawback of this technique. It is normally 20 min and can be reduced even more if dyes exist, for the existence of salts, temperature and pH affects the stability. The short half-life will result in high cost since continuous ozonation will be needed. The effluent pH must be cautiously observed in the case of alkaline conditions since ozone decomposition will be sped up. Utilizing irradiation or a membrane filtration method would attain better outcomes [23].

Photochemical. Using this technique, dye particles will be degraded to carbon dioxide and water molecules by ultra violet treatment when H_2O_2 is present [30]. The generation of great concentrations of hydroxyl radicals leads to degradation. Chemicals like H_2O_2 are activated by using ultra violet light which its intensity together with pH, dye structure and composition affect the dye removal rate. A batch or continuous column may be used for this. The generation of extra by-products like halides, metals, organic and inorganic acids may occur based on primary substances and the decolorization treatment range [31]. Advantages of such treatment include the elimination of sludge and reduction of foul odors. Organic substances are chemically oxidized because of the degradation of H_2O_2 into two hydroxy radicals by ultra violet light [23].

Sodium hypochlorite. In this technique, the chloride ion is used to attack the amino group of the dye particle.

Azo bond cleavage will be started off and sped up. Increment in Cl concentration results in having higher discoloration, so this method is undesirable for

disperse dyes. Discharging Cl and carcinogenic aromatic amines into water bodies results in adverse effects on the environment making this method unfavorable to use [23].

Electrochemical destruction. Developed in the mid 1990's, this method is considered novel in the dye removal industry. It is considered an effective technique since there is no need to use chemicals and there is no sludge accumulation. The treated effluent is safe to be discharged into water bodies since the metabolites are normally not dangerous. The price of electricity utilized is equivalent to the chemicals cost and decreasing flow rates result in increasing the dye removal. This method is economic and efficient to use for dyes removal, color removal and recalcitrant pollutants degradation [32].

2.3.3. Physical treatment methods. Physical treatment techniques are typically simple techniques generally achieved by the mass transfer process. These methods do not need as much chemicals as the biological and chemical methods require and do not deal with living things, so they are more anticipated than the other two techniques. Traditional methods include coagulation or flocculation, ion exchange, membrane filtration and adsorption. Physical dye removal methods have a removal percentage ranging from 86.8 to 99% with the adsorption method ranking the highest [3].

Membrane filtration. A membrane is a fine coat of semi-porous material that splits up matter when applying a driving force towards the membrane [33]. This technique is capable of clearing, concentrating, and removing dye constantly from wastewater. It includes microfiltration, ultrafiltration, nanofiltration and reverse osmosis. Because of the big pore size of microfiltration, it is not useful for wastewater treatment. Even though ultrafiltration and nanofiltration methods are efficient in removing all categories of dyes, dye particles result in continual blocking of the membrane pores limiting the use of the separation method for dye wastewater treatment.

In reverse osmosis, by applying pressure, water is forced through an impermeable membrane that discards salt better than discarding non-ionized weak acids and bases. It is capable of decoloring and desalting dye effluent resulting in

almost clear water that can be used for recycling [14]. Some of the advantages of this method are that it is temperature resistant and does not consume chemicals. The major disadvantages include high capital cost, high operating pressures, considerable energy utilization and the membrane's high price and short life [14], [23].

Ion exchange. Ion exchange is a method that involves the interchange of an ion from a mixture for an equivalently charged ion connected to a static solid particle [14]. Far and away, ion exchange has been widely used in water softening, which is the removal of calcium, magnesium and other metal cations in exchange for sodium. This technique has not been commonly utilized for dye wastewater treatment since ion exchangers cannot conciliate a broad extent of dyes. The dye effluent goes through the ion exchange resin till saturation of the exchange sites is accomplished. This method works best for the removal of anion and cation dyes. Successful regeneration of adsorbent after utilization, recovery of solvent and elimination of soluble dyes are some of the features of this technique. The main drawback of this method is the high cost. The high price of organic solvents and not being suitable for removal of disperse dyes make this method not very effective [23].

Adsorption. Adsorption stands out as one of the favorite dye removal methods among the countless tried-and-tested techniques because of its excelling capability to remove nearly any kind of dyes [25], [34]. Purification of industrial wastewater or cleaning drinking water can also be achieved by this method. Traditional techniques have been proven ineffective in removing synthetic dyes from dye effluent since they are incapable of entirely removing the dye from wastewater. So, adsorption is considered one of the best possible dye removal techniques as higher treated water quality is generated compared to other techniques. Adsorption is a non-reactive, mass transfer process illustrated by the cumulation of a material at the interface between two phases (liquid-solid interface or gas-solid interface). Adsorbate is the material that piles up at the interface while adsorbent is the solid on which adsorption happens [35].

Adsorption can be divided into two categories: chemical sorption and physical sorption. Chemical adsorption, or in other words, chemisorption takes place when strong chemical connections between adsorbate molecules to the surface of adsorbent

are formed which is normally because of the electrons exchange and therefore it is considered an irreversible process. When there are weak van der Waals intramolecular bonds between the adsorbate and adsorbent, physical adsorption or physisorption takes place. This kind of adsorption is mostly considered reversible [9]. Adsorption is an extraordinary method for removing dyes due to its ease of operation and no need for further specific equipment. Moreover, there is no need for pre-treatment for the launch of the process and no dangerous substance will be produced at the end [3]. The high price of adsorbents is a main drawback of this method, but since new adsorbents with low price and equal efficiency have come to light, this technique became a low-cost process of dye removal around the world [36]. It is important to have a convenient design of the adsorption system to assure a high quality of treated wastewater is being produced [9]. The parameters that impact the adsorption efficiency are the interaction between the adsorbate and adsorbent, dye concentration, adsorbent features such as dosage, surface area and particle size, and the temperature and pH of the mixture [3], [9].

An adsorbent is a permeable insoluble material that can seize and restrict adsorbate particles onto itself. It is the most important part of the process. The essential features of a good adsorbent include its adsorption capacity and surface area [23]. A larger surface area suggests a more permeable adsorbent assuring a high adsorption capacity [37]. Other desired characteristics include short adsorption period, variety in ejecting a broad extent of pollutants, and ability to operate in different dye concentrations, pH and temperature [38]. A wide variety of adsorbents have been used to remove different types of dyes from water and wastewater. Some of them include: activated carbon, zeolites and metal organic framework (MOFs).

Activated Carbon. Nowadays, using activated carbon-based adsorbents in the adsorption process is more common and effective than using other adsorbents [9], [25], [38]. Activated carbon can be generated from any carbon rich substance and it has a broad range of surface areas reaching a maximum of 2000 mg/g.

Appealing features this adsorbent include are its capability of regeneration, affinity with different components and its huge surface area [39]. Being from the first and most dynamic adsorbents, activated carbon can be obtained from any

carbonaceous matter like coal, sawdust, palm kernel shell, cow dung and date-pits. Many researchers have used coal based activated carbon, or in other words, commercial activated carbon for the removal of a broad range of dye particles from wastewater. Activated carbon is also quite effective in removing heavy metals and other dangerous pollutants [40], [41]. The issue with commercial activated carbon is that coal is a costly non-renewable energy resource since it is a fossil fuel and soon may be discontinued. To cope with this, renewable sources such as biomass, natural and waste materials are being utilized these days to produce activated carbon as they are also cheap in addition to being renewable [13], [34]. Characteristics of activated carbon obtained from various raw materials vary as well. There are two straightforward processes to produce activated carbon. Firstly, the chosen carbon rich raw material is carbonized in a static surrounding at a 1000 °C temperature. Secondly, a proper chemical is used to activate the carbonized material [36].

Two techniques are used to activate carbon, either chemically or physically and a comparison between these two methods is presented in Table 5. Using waste material to produce activated carbon will assist in the reduction of environmental pollution and the use of raw materials. Activated carbon adsorption capacity is affected by its pore size and structure, surface chemistry and charge, the raw material utilized, its carbon composition, and the treatment technique and its circumstances [34], [38]. A perfect activated carbon must have a large surface area, big pores, and has a multipored design. Small molecules that are smaller than 1 nm are removed by using microporous activated carbon, while big molecules that are bigger than 1 nm are removed by macro porous or mesoporous activated carbon [42]. Activated carbon in the powdered form is what is commonly used in removing dyes since they have higher surface area than other forms like fibers, blocks, pellets and grains [13]. The van der Waals forces help with the adsorption onto activated carbon. This method is proven to achieve a complete removal of all kinds of dye molecules. Adsorptive characteristics of the activated carbon will slowly get weak after constant dye removal. The adsorption capacity of activated carbon won't be the same as the new one as their pores will not have the ability to take in further dye particles any more. Nonetheless, advancement in technology made it possible to regenerate activated carbon by reactivating it [43]. The drawback of such technology is the carbon loss and

the adsorption capacity reduction. Table 6 shows that activated carbon will have high surface areas and effective dye removal when obtained from cheap raw materials resulting in cheap overall process cost [44].

Table 4: Comparison between chemical and physical carbon activation processes [3]

| Method | Chemical Activation | Physical Activation |
|------------------------|--|--|
| Activation Time | Short | Long |
| By-products | None | Non-porous char |
| Number of steps | 1 (2 steps implemented simultaneously) | 2 |
| Requirement | Carbon activation chemicals (H ₃ PO ₄ , KOH, K ₂ CO ₃ , NaOH, ZnCl ₂) and nitrogen | Inert and oxidising gases |
| Steps | 1.Raw material saturated with chemicals 2.Heated under flowing nitrogen gas | 1.Pyrolysis process to carbonize raw material 2. Use of air, carbon dioxide, steam or a mixture of oxidising gases for activation |
| Surrounding | Inert (nitrogen) | |
| Temperature | Low (450-900 °C) | High (600-1200 °C) |
| Washing | Needed (due to use of chemicals that must be removed) | Not needed (no use of chemicals) |
| Features | Less burnt activated carbon | -Mesoporous structure -Convenient for dye adsorption -Larger pore size |
| End product | Activated carbon | |

Table 5: Adsorption capacity and surface areas for different types of activated carbon [3]

| Activated Carbon | Adsorption capacity (mg/g) | Surface area ($\frac{m^2}{g}$) |
|-------------------------|-----------------------------------|--|
| Almond shell | 1.33 | 783 |
| Apricot shell | 4.11 | 783 |
| Bagasse | 391 | 1433 |
| Bamboo | 454.2 | 1896 |
| Cashew nut shell | 476 | 984 |
| Commercial | 980.3 | 650 |
| Corncob | 1060 | 943 |
| Granule | 57.47 | 1100 |
| Groundnut shell | 222.2 | 1114 |
| Hazelnut shell | 8.82 | 793 |
| Pine sawdust | 370.37 | 1390 |
| Pinewood | 1176 | 902 |
| Plum kernel | 904 | 1162 |
| Sawdust | 183.8 | 516.3 |
| Treated rice husk | 290 | 2516 |
| Walnut shell | 3.53 | 774 |
| Waste newspaper | 390 | 1740 |

Zeolites. Zeolites are extremely permeable aluminosilicates with various bore structures. They are composed of a three-dimensional framework, with a negatively charged grid. Cations that can be exchanged with specific cations in mixtures balance the negative charge. They normally contain silicon, aluminum, and oxygen. Figure 2 shows the basic zeolite structure. Zeolites can be found naturally, with over than 40 natural type, or made by synthesis [14]. Clinoptilolite is the amplest and most widely researched zeolite, which is a mineral of the heulandite group. Its structure consists of 8-10 membered rings in open channels with ease of access having high selectivity for specific pollutants. They are considered appealing adsorbents due to their comparatively large fixed surface areas, ion selectivity, high ion exchange capacity and low cost. When there is a requirement for sorptive applications, zeolites are being excessively employed in these areas. Zeolites have the ability to remove trace amounts of pollutants like heavy metal ions, dyes and phenols due to their structures that enable ion exchange. Highly low sorptive capacities of raw clinoptilolite made it a bad choice for removing reactive dyes [9], [20]. Woolard et al. [45] transformed fly ash into zeolites by treating raw ash hydrothermally with base. The considerable increase in surface area and cation exchange capacity were bearable by the produced material unlike raw ash. Also, it had higher affinity for cationic dyes sorption than raw ash, which is due to the increase in surface area instead of a certain interaction [34]. One of the disadvantages of zeolites is their low permeability which needs an additional support when utilized in column units. This method is complicated due to the zeolites porous structure and surface imperfections. Zeolites adsorption characteristics; however, typically develop from ion exchange abilities, like clay. Despite zeolites being not very effective in removing dyes as clay materials are, their high availability and low price make up for the related disadvantages [9], [20].

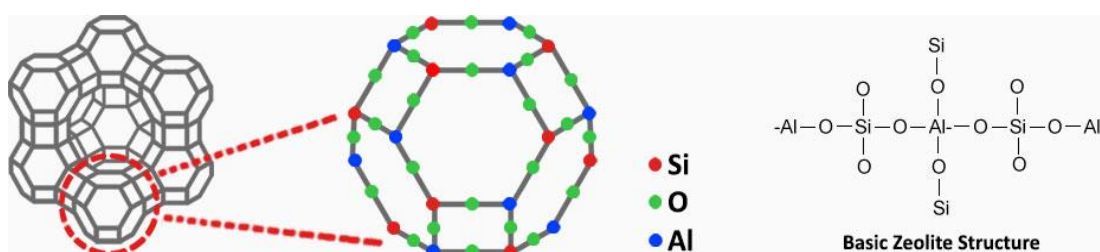


Figure 2: Zeolite structure [46].

Metal Organic Frameworks (MOFs). Metal Organic Frameworks are organic-inorganic crossbred solids with infinite and consistent crystalline assortment networks composed of metal clusters and organic linkers. In 1995, the first MOF with enduring porosity was announced. Throughout the evolution of this new kind of crossbred solids, there was not an approved criterion for nomenclature, so many names were suggested and are in use. Some of these names involve porous coordination polymers [47], microporous coordination polymers [48], zeolite-like MOFs [49] and porous coordination networks [50]. Coordination bonds are used to connect the organic and inorganic units. Usually, the inorganic units are metal ions or metal cluster and the organic units, which can also be named linkers or ligands are di-, tri-, or tetradentate organic linkers like carboxylates or organic anions such as sulfonate and phosphonate compounds [51]. Figure 3 shows the chemical structure of a classic MOF, MOF-5. The organic linkers are groups that can give various single pairs of electrons to the metal ions, while the metal ions are formed with empty orbital shells that can take these single pairs of electrons to create a metal organic framework material [52]. Figure 4 presents the organic linkers used for MOF synthesis.

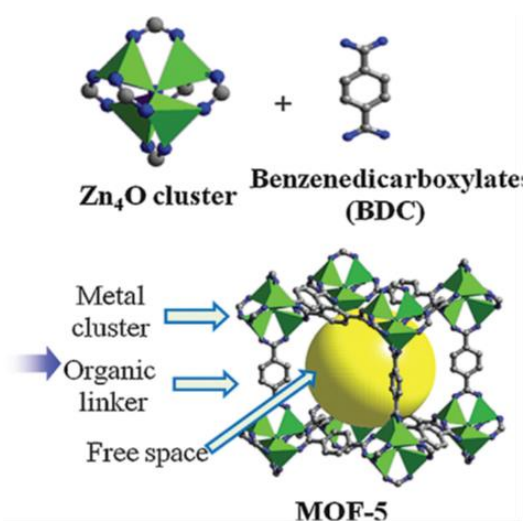


Figure 3: Chemical structure of a classic MOF, MOF-5 [53].

Great attention has been drawn to MOFs in academia and industry due to their versatility and possible utilizations. Since MOFs have possible applications in several areas, the research and number of publications associated to MOFs has grown quickly [53].

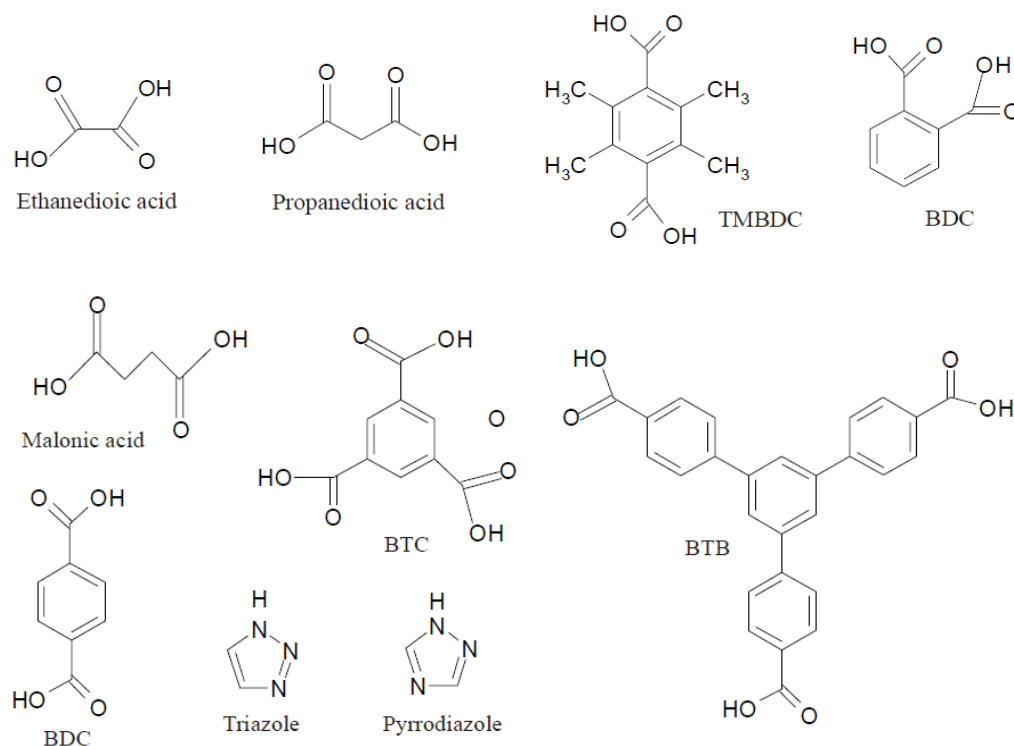


Figure 4: Organic linkers used for MOF synthesis [52].

There are various appealing features that make MOFs distinctive and unlike other traditional permeable solids. These contain (1) straightforward and convenient synthesis compared with zeolites [54]. (2) large surface areas and adjustable porosities [55]. (3) the existence of coordinatively unsaturated sites (CUSs) or open metal sites (OMSs) [56] and (4) the capability to incarnate certain operations / active species without changing the framework topology [57]. Attractive characteristics of MOFs include their structure that is easy to synthesize, topologically varied and esthetically satisfying with neutral skeleton [55]. Throughout the making of MOFs, the solvent serves out as the prime mold unlike zeolites where organic or inorganic molds are needed. Furthermore, there are normally weak interactions between the solvents and the framework, which makes it essential for acquiring final products with complete neutral frameworks and available pores at relatively low temperatures [54]. Another appealing characteristic of MOFs is that different metal cations can take part in the development of different MOFs unlike zeolites where just a small number of cations like Si, Al and P are capable of creating such structures [55]. The features of MOFs are controllable to some range to attain required purposes or to accomplish enhanced

performances by consistently and intentionally tuning their frameworks and operations; for instance, the surface area, pore size or shape are tunable by changing the linkage of the inorganic moiety and the organic linker's quality. Certain examples are three zirconium-based MOFs, specifically UiO-66 (Zr-BDC), UiO-67 (Zr-BPDC) and UiO-68 (Zr-TPDC) that have surface areas 1187, 3000, and 4170 m^2/g , respectively [58]. Due to altering the organic linker, a vast increase in the surface area is attained [58]. Likewise, when reacting with the same organic linker, various metal clusters compose analogous topological structures with various physiochemical features like CUSs or OMSs, stability, and Lewis acidities. For example, CPO-27 MOF have the framework Me-DHTP when the organic linker Me reacts with the different metal clusters $Co^{2+}, Ni^{2+}, Fe^{2+}, Mn^{2+}, Zn^{2+}$. Another interesting characteristic of MOFs is their potential to adjust their physiochemical characteristics after their formation [59]. Several MOFs are adequately strong and permeable so that post-synthetic modification (PSM) is achieved without losing the original framework topology. The usage of post synthetic-modification (PSM) like post-functionalization of amine groups with sultones [59] or post-synthetic framework sulfonation [60] helped to convey acidic or basic functionalities to MOFs. Furthermore, adjustment of MOF characteristics can be done by loading active metals like Cu, Ag, or Pd or active substances like polyoxometalates or sulfated zirconia or by creating composites. A critical problem that is faced when dealing with MOFs is their water stability. Effort has been made to solve this issue since water instability (in liquid and vapor state) can create a significant obstruction to use multiple types of MOFs in functional implementations [61]. Upon water exposure, several MOFs like MOF-5 and MIL-101-V experience degradation through linkers displacement or hydrolysis. Nevertheless, different MOFs like MIL-100 (Al, Cr, Fe) and ZIF-8 have high water stability and can be used for purifying water or adsorption in water. To improve water stability of MOFs, techniques like fluorination, composite formation, and incorporating water repellent functional groups are being used. So, this problem might not be that severe for MOFs applications [51].

For the last two decades, there has been an ongoing research on MOFs due to their fascinating chemistry, distinctive features and most importantly their multilateral possible applications. Some of these applications include hydrogen and methane

storage, which can be utilized as fuels for static and transportation implementations. Another application is in the medical research, especially in drug delivery and biomedicine, where MOFs are utilized in encapsulation of drugs and imaging and analytical applications. MOFs are also used in adsorption/ storage in gas and liquid phases such as CO₂ capture and sequestration. In catalysis, they are used as heterogeneous catalysts due to their large surface areas and adjustable pore surface implementations. They are also utilized in electric and electronic equipment depending on their conductivities [62]. Separation of chemicals, chemical sensing, polymerization, luminescence and magnetism are further applications where MOFs are used [63].

Haque et al. have done some innovative studies on using MOFs for dye removal. In 2010, the dye adsorption performances of MOFs were examined for the first time [64]. In order to remove the anionic dye Methyl Orange from aqueous solutions, two standard highly permeable MOF materials based on chromium-benzenedicarboxylates (Cr-BDC), namely MIL-53-Cr and MIL-101-Cr, where MIL corresponds to Material of Institute Lavoisier and some other adjusted MOFs were utilized [65]. The results demonstrated that high porosity, big pore sizes and electrostatic interactions were accountable for the improved adsorption capacity and rate and that they were considerably greater than activated carbon for the removal of the same dye. This corresponded to MIL-101 being a better option than MIL-53 for the removal of MO. In another study, Haque et al. investigated the simultaneous removal of anionic and cationic dyes through adsorption. The adsorption of Methyl Orange as an anionic dye and Methylene Blue as a cationic dye was studied by using an iron-based MOF, namely iron terephthalate MOF-235. The results showed that the adsorption capacities of MO and MB with MOF-235 were 477 and 187 mg g⁻¹, respectively and were much higher than those of Activated Carbon. A further study proposed Zeolitic imidazole frameworks (ZIFs), a recently developed type of MOFs, for the adsorption of Malachite Green (MG) in water. ZIF-67 was chosen due to its water stability and simple synthesis. The adsorption capacity of MG with ZIF-67 was as high as 2430 mg/g at 20°C, which can be enhanced by increasing the temperature. This adsorption capacity was nearly 10 times of those of traditional adsorbents including activated carbon and biopolymers [66]. The adsorption capacities of Malachite Green and Methyl Orange with various MOFs are demonstrated in Table 6.

If MOFs can be regenerated and reused for the MG adsorption, the cost can be significantly reduced, and the adsorption process becomes even more competitive. Lin et al. [66] investigated the recyclability of ZIF-67 for the MG adsorption. To regenerate the spent ZIF-67, an ethanol-washing method was employed owing to its simplicity and inexpensiveness. After the first-cycle regeneration, ZIF-67 still exhibited a comparable adsorption capacity, showing that the ethanol-washing was a feasible and effective technique to remove MG from the spent ZIF-67. As the regeneration cycle increased, the adsorption capacity of ZIF-67 remained similar and no significant loss was observed. After four regeneration cycles, ZIF-67 could still exhibit 95% of the original capacity of ZIF-67. This suggests that ZIF-67 can be readily and straightforwardly regenerated and the adsorption capacity can remain almost the same, even up to 4 cycles. Depending on the prior attractive returns, it can be deduced that MOFs are better adsorbents than activated carbons and zeolites due to their higher adsorption capacities as well as their higher stability and regenerability. Thus, MOFs are considered promising adsorbents for dye removal from wastewater.

Table 6: Malachite Green and Methyl Orange adsorption capacities with various MOFs

| MOF | Temperature (°C) | Maximum adsorption capacity, (mg/g) | References |
|--|------------------|-------------------------------------|------------|
| Malachite Green (MG) | | | |
| ZIF-67 | 20 | 2430 | [66] |
| Cu- MOF | 25 | 38.01 | [67] |
| Cu-MOFs/Fe ₃ O ₄ | 25 | 113.67 | [68] |
| MIL-100(Fe) | 25 | 146 | [69] |
| MIL-53(Al)-NH ₂ | 25 | 188.6 | [70] |
| MIL-100-SO ₃ H | 30 | 528 | [71] |
| NH ₂ -MIL-101(Al) | 30 | 274 | [72] |
| Methyl Orange (MO) | | | |
| MIL-53(Cr) | 25 | 57.9 | [64] |
| MIL-101(Cr) | 25 | 114 | [64] |
| MOF-235 | 25 | 477 | [73] |
| MIL-68(Al) | 35 | 341.3 | [74] |
| MIL-100(Cr) | 30 | 211.8 | [75] |
| MIL-100(Fe) | 30 | 1045.2 | [75] |
| NH ₂ -MIL-101(Al) | 30 | 188 | [76] |

Chapter 3. Experimental Work and Methodology

3.1. Materials

MIL-53(Al) was supplied by Sigma-Aldrich (USA) under trademark Basolite® A100 and was utilized without additional purification. Aluminum (III)-based MOF (MIL-53(Al)) is among the most attractive MOFs because of its breathing effect and being stable both in acidic and neutral aqueous mixtures [70]. It has also been extensively studied for water treatment and hydrogen storage [77].

Malachite Green is a cationic dye classified in the triphenylmethane class, dissolvable in water, and is widely utilized for the dyeing of silk, cotton, paper and leather products [16]. MG was purchased from Sigma Aldrich (USA) as 10,000 mg/L stock solution. Methyl Orange is a common anionic dye widely utilized in textile, printing, and laboratory experiments [78]. MO was purchased from LabChem (USA) as 1000 mg/L stock solution. Various concentrations of MG and MO solutions were prepared by subsequent dilution using distilled water. Hydrochloric acid (37%) and sodium hydroxide (98%) were utilized for pH alteration for the preparation of 1.0 M aqueous solutions of HCl and NaOH. Ethanol (70%) was used for the renderability of the MOF (MIL-53(Al)).

3.2. Adsorption Experiments

For the single-dye adsorption, the aqueous solutions were prepared by consecutive dilution of the stock solution of MG or MO with distilled water. While, for the binary-dye (MG-MO) adsorption, certain amounts of stock solutions of MG and MO were diluted all together with distilled water to prepare the aqueous mixtures. A UV-Vis Spectrophotometer (Thermo Scientific, Evolution 60s, USA) was used to measure the absorbance of the prepared solutions in order to identify the concentration of MO and MG by using their calibration curves shown in Figure 5 and 6, respectively. The calibration curve for each dye was attained by using a set of standard solutions at different concentrations (1-30 mg/L) and was found to be linear and consistent over the utilized concentration range. This was done by serial dilutions of the stock solution for both MG and MO, for which no artificial adjustment of the pH was made. The batch experiment was performed by adding certain amounts of MOF adsorbent to 50 mL beakers that contained 50 mL MG, MO or MG-MO solutions with various initial concentrations (7-13 mg/L) at a certain pH and

temperature. To prevent possible water vaporization, these beakers were sealed and then a magnetic stir plate was used to mix the solutions and make sure they were homogeneous in consistency and temperature. The solutions were then kept for a certain amount of time (5 min to 3 hr) to guarantee complete adsorption and achieve equilibrium. Using a 5 mL syringe, the samples were taken then filtered by membrane filters (Nylon, 13 mm diameter, 0.45 μm pore size). Following that, the UV-Vis spectrophotometer was used to measure the residual concentrations of Malachite Green and Methyl Orange in the sample at maximum wavelengths of 617 and 464 nm, respectively in case of single-dye solutions. For binary-dye solutions, the maximum wavelength for MO shifted to 430 nm while stayed the same for MG (617 nm). Furthermore, every experiment was performed in replicate and the standard deviation values were recorded.

The amounts of adsorbed MG and MO per unit mass of the adsorbent at time t , (q_t (mg/L)) and at equilibrium, (q_e (mg/L)) were calculated by equations (1) & (2), respectively.

$$q_t = \frac{(C_o - C_t) \times V}{m} \quad (1)$$

$$q_e = \frac{(C_o - C_e) \times V}{m} \quad (2)$$

where C_o is the initial concentration of MG or MO solution (mg/L), C_t is the residual concentration of MG or MO solution at time t (mg/L), C_e is the residual concentration of MG or MO solution at equilibrium (mg/L), V is the total volume of the solution (L), and m is the mass of the MOF used (mg).

The percentage dye removal of the MOF was determined by equation (3).

$$\% \text{Removal} = \frac{(C_o - C_t)}{C_o} \times 100 \quad (3)$$

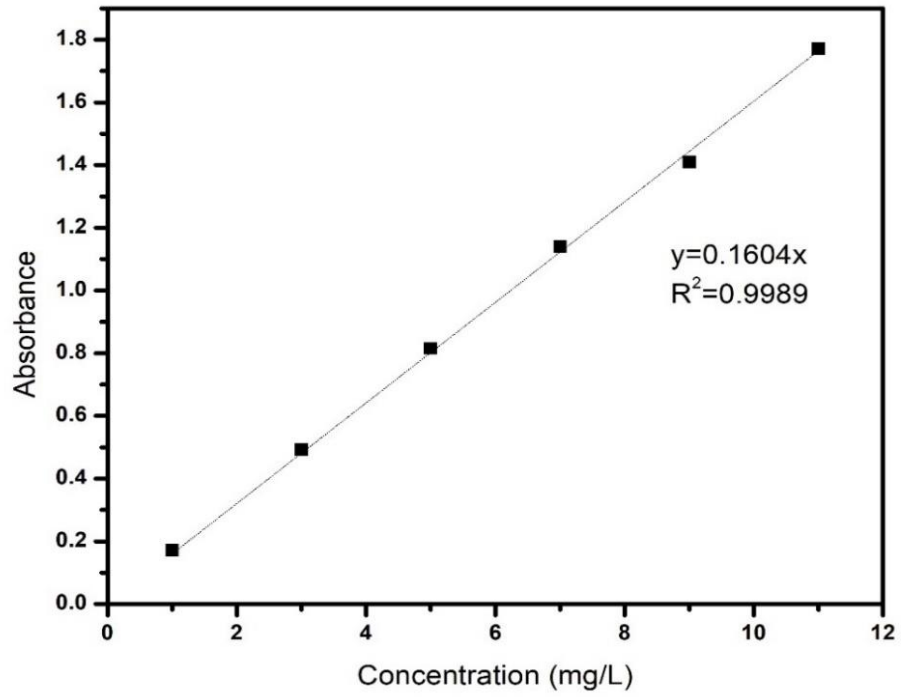


Figure 5: Calibration curve for MG solution.

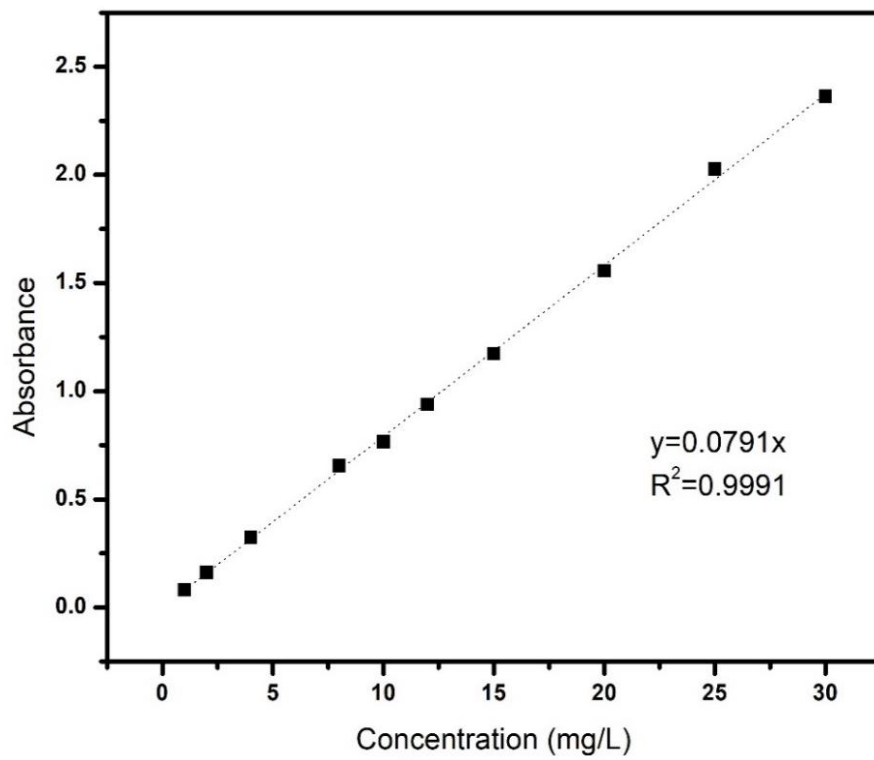


Figure 6: Calibration curve for MO solution.

3.3. Characterization

Multiple methods were used for the characterization of MIL-53(Al) in order to study the effect of adsorption of MG and MO. The crystalline structure of the MOF was determined by X-ray powder diffraction (XRD). A Bruker advance device was used to collect XRD samples with Cu K α radiation and a linear detector (Germany, AXS D8). The scanning range over which the measurements were carried out was of 5-60° with a 0.03° step size.

Fourier transform infrared spectroscopy (FT-IR) were performed using FTIR spectrophotometer (PerkinElmer, USA) at 4000-400 cm⁻¹ scanning wavelength range by utilizing KBr pellet pressing technique. Signal-averaging of 10 scans were taken at a 1.0 cm⁻¹ resolution.

The work done by Milonjić et al. was used to determine the point of zero charge, pH_{pzc}, of MIL-53(Al) [79]. The background electrolyte that was used in this method was sodium chloride (NaCl), having a concentration of 0.01 M. For the adjustment of the initial pH values (pH_i) in the range of 2 to 10, small amounts of 1M HCl or 1 M NaOH were *added* to the solutions and measured using a portable pH meter (HANNA Instruments, USA). Conical flasks of 100 mL were used, each containing 50 mL of 0.01 M NaCl solution. Then, 100 mg of the MOF MIL-53(Al) was added to every flask before firmly sealing them. After that came the process of shaking the suspensions irregularly and keeping them for 48 hours at room temperature so that they reach equilibrium. After 48 h, the final pH values were measured and were used to find the difference between them and the initial pH values. A graph of the difference in pH values (ΔpH) against the initial pH values (pH_i) was plotted, in which pH_{pzc} was determined when (ΔpH) was equal to zero.

3.4. Adsorption Kinetics

Kinetic models are defined by using the controlling techniques of adsorption like diffusion control, chemical reaction or mass transfer coefficient. When it comes to selecting the finest modes of operation for the full-scale adsorption approach, the kinetics of dye adsorption onto adsorbent substances is an essential requirement. When coming up with the adsorption system, it is essential to take this rate into account, which can be calculated from the kinetic study. The solute uptake rate is demonstrated by the kinetics study and can be clearly used for controlling the dye's

residence time at the mixture interface. Therefore, various kinetic models were used to study the MO and MG kinetics onto MOF MIL-53(Al). The same procedure described earlier was used here. At certain time intervals, samples were taken from the solutions that had initial concentrations of 7-13 mg/L in order to determine the concentrations of MO and MG with time. Four kinetic models were used to investigate the data. The pseudo first-order (PFO) model [19], the pseudo second-order (PSO) model [80], elovich model [81], and intraparticle diffusion model [82] were studied in this work and can be demonstrated by equations (4-7).

Pseudo first-order model

$$q_t = q_e(1 - e^{-k_1 t}) \quad (4)$$

Pseudo second-order model

$$q_t = \frac{k_2 q_e^2 t}{1 + k_2 q_e t} \quad (5)$$

Elovich model

$$q_t = \frac{1}{\beta} \ln(1 + \alpha \beta t) \quad (6)$$

Where q_e and q_t (mg.g^{-1}) are the adsorption capacity of MG or MO at equilibrium and at specific time t (min), respectively, k_1 (min^{-1}) represents the rate constant of the first-order kinetic, k_2 ($\text{g.mg}^{-1}.\text{min}^{-1}$) is the second-order kinetic constant, α ($\text{mg.g}^{-1}.\text{min}^{-1}$) is the initial adsorption rate, and β (g.mg^{-1}) is a desorption constant associated to the degree of covered surface and the chemisorption activation energy. Non-linear regression was used to find out the kinetic parameters.

Intraparticle Diffusion model

$$q_t = k_{id} t^{0.5} + C \quad (7)$$

Where k_{id} ($\text{mg.g}^{-1}.\text{min}^{-0.5}$) is the rate constant, and C (mg.g^{-1}) is the boundary layer thickness. This mechanism is regarded as rate-limiting step when a graph of q_t against $t^{0.5}$ gives a linear plot that goes through the origin [83].

3.5. Adsorption Isotherms

The adsorption isotherm is crucial for the clarification of the interaction between the adsorbent and adsorbate and to give an overall idea of the adsorption capacity. The isotherm models play a huge part in comprehending the adsorption mechanism. The surface phase can be either monolayer or multilayer [84]. It is crucial to report the adsorption process using the most proper model by fitting the isotherm data to various isotherm models. The isotherm experiments were carried out in 50-mL conical flasks containing 50 mL of MO or MG solution with initial concentration ranging from 13 to 250 mg/L, which were sealed and maintained at 25, 35 or 65 °C before the addition of 10 mg of MIL-53(Al). Langmuir [85] and Freundlich [85] were the models that were used to analyze the experimental data.

The Langmuir model is developed on the assumption that homogeneous sites of the adsorbent will be covered with a monolayer of the adsorbate, in which the adsorbed molecules don't interact with each other [86]. This model is described by equation (8).

$$q_e = \frac{q_m K_L C_e}{1 + K_L C_e} \quad (8)$$

Where q_m is the maximum adsorption capacity when the adsorbates are completely covering the monolayer surface (mg/g), and K_L is the Langmuir constant (L/mg) linked to the adsorption energy (L/mg).

The Freundlich isotherm assumes a heterogeneous and multilayer adsorption [85]. The surface on which the adsorption takes place is considered to have different accessible sites with various adsorption energies [84].

The Freundlich isotherm is given by equation (9).

$$q_e = k_F C_e^{\frac{1}{n}} \quad (9)$$

Where k_F is the Freundlich constant associated with the adsorbent capacity $((\text{mg}\cdot\text{g}^{-1})(\text{L}\cdot\text{mg}^{-1})^{1/n})$ and n represents the intensity of the adsorption driving force. The higher the value of n , the higher the adsorption feasibility. Since Freundlich isotherm

considers both monolayer and multilayer adsorption, both chemical and physical adsorption have to be accounted when using this model [70].

A dimensionless separation factor (R_L) can be used to represent the adsorption favorability in a particular extent of concentration as shown in equation (10).

$$R_L = \frac{1}{(1 + K_L C_o)} \quad (10)$$

The isotherm type is determined by this value. It is regarded to be linear if $R_L = 1$, irreversible if $R_L = 0$, favorable if R_L is between 0 and 1, and unfavorable if $R_L > 1$ [18].

3.6. Adsorption Thermodynamics

Temperature dependent adsorption isotherms are used to identify the thermodynamics parameters in order to study the adsorption process. They determine the relationship between the adsorbent and the adsorbate and indicate the practicality and spontaneous nature of the adsorption mechanism. The adsorption data of MG and MO on MIL-53(Al) at different temperatures were used to calculate Gibbs free energy ($\Delta G^\circ, kJ/mol$), standard enthalpy ($\Delta H^\circ, kJ/mol$), and standard entropy ($\Delta S^\circ, J/mol K$) according to the following formulas (11) and (12).

$$\Delta G^\circ = -RT \ln(K_{eq}) \quad (11)$$

$$\ln(K_{eq}) = \frac{\Delta S^\circ}{R} - \frac{\Delta H^\circ}{RT} \quad (12)$$

Where R is the universal gas constant, and K_{eq} is the thermodynamic equilibrium constant. By plotting $\ln(K_{eq})$ against $1/T$, ΔH° and ΔS° can be determined from the slope and intercept of the linear graph, respectively according to equation. Following this, the value of ΔG° at a specific temperature is attained from equation (11).

3.7. Selectivity of Binary-Dye Adsorption

For binary-dye adsorption, equimolar MG/MO solutions were prepared with initial concentrations in the range of 7-13 mg.L⁻¹ for each dye and added to 50 ml beakers, to which MIL-53(Al) was added in amounts of 10 – 50 mg. The selectivity (dimensionless) of MIL-53(Al) can be calculated according to equation (13) [87].

$$Selectivity = \frac{q_{e,1}/C_{e,1}}{q_{e,2}/C_{e,2}} \quad (13)$$

where $C_{e,1}$ and $C_{e,2}$ are the solution concentrations of dye 1 and dye 2 at equilibrium ($mg \cdot L^{-1}$), respectively. $q_{e,1}$ and $q_{e,2}$ are adsorption capacities of dye 1 and dye 2 at equilibrium ($mg \cdot g^{-1}$), respectively.

3.8. Factorial Design

A factorial design is used for the sake of studying how more than one factor can affect the adsorption process, as it requires to alter all variables simultaneously from a single experiment to another [88]. This is because of the effects that these factors have on each other, which is considered to be very common to occur [89]. Factorial design is believed to be an effective way to define the ultimate response from a series of measured responses [90]. Some of the advantages of this approach are that it is less costly and more trusted outcomes are acquired. Other advantages may include the less time needed to complete the experiment and being probably the most straightforward kind of statistical analysis [91].

In this work, the primary impacts of experimental factors such as adsorbent dosage, MG initial concentration and MO initial concentration were investigated as well as the interactions between them by using a full factorial design mechanism. This method includes runs at each probable group with every factor's specified lower and upper level. Specifically, three independent factors were utilized, that is, amount of MOF (A), MG initial concentration (B) and MO initial concentration (C), while the response was the adsorption capacity of each of the dyes in the binary solution. In order to develop this design, N^k experiments are needed, where k represents how many factors are utilized in the design and N describes how many levels are there. The impacts of these primary factors and their interactions were studied using a 2^3 full factorial design. Experimental error was estimated by duplicate establishment of every experiment in order to define the statistical importance of the effects. Possible sets of experiments were performed randomly with several levels of factors. Minitab 17 statistical software was used to investigate the outcomes of the design and examine the effects, parameters and statistical plots. It was used to investigate the interactions between the variables and the primary impacts of dye adsorptions were determined in reliance on the P value that was of >95% of confidence level.

Chapter 4. Results and Analysis

In this chapter, the adsorption of the cationic dye (Malachite Green) and the anionic dye (Methyl Orange) over the Metal Organic Framework (MIL-53(Al)) is reported. At present, the focus of most researchers when studying adsorption on MOFs is to investigate the removal of a single dye, whether cationic or anionic, from the solution. The research on the concurrent adsorption of both anionic and cationic dyes from a solution on MOFs is not readily accomplished [19]. The crystalline structure, framework and morphology of MIL-53(Al) were studied by X-ray diffraction (XRD), Fourier transform infrared spectroscopy (FT-IR), and scanning electron microscope (SEM) in order to understand how adsorption affects such characteristics. Moreover, a variety of experimental factors such as initial dye concentration, contact time, pH, MOF dosage and temperature were investigated in MG and MO adsorption experiments. The adsorption kinetics, equilibrium isotherms, and adsorption thermodynamics were evaluated so that the adsorption mechanism of the molecules of the different dyes onto the MOF can be understood. In addition, selective removal of each dye from MG-MO mixture was studied. The regeneration of the MOF (MIL-53 (Al)) was examined as well. Finally, the significance of factors such as the MOF dosage and each dye initial concentration was assessed by developing a 2^3 full factorial design.

4.1. Characterization Tests

The XRD patterns of MIL-53 (Al) before and after the adsorption process of MG and MO dyes are shown in Figure 7. It can be seen that the commercial XRD patterns of the MOF's samples are consistent with the simulated ones reported in literature for the as-synthesized samples prepared in lab [70], [77], [92].

The XRD spectra of MIL-53(Al) present six characteristic peaks at 2θ of 8.98° , 12.72° , 15.26° , 17.78° , 25.46° , and 33° . These peaks are intense and precise, suggesting that MIL-53(Al) has a good crystallinity as well as a fine structure. It is observed that there is no major change in the diffraction patterns of MIL-53(Al) after adsorption of MG and MO dyes when compared to the one before the adsorption process. This implies the conservation of the crystalline structure of MIL-53(Al) after being exposed to MG and MO dyes for certain periods of time.

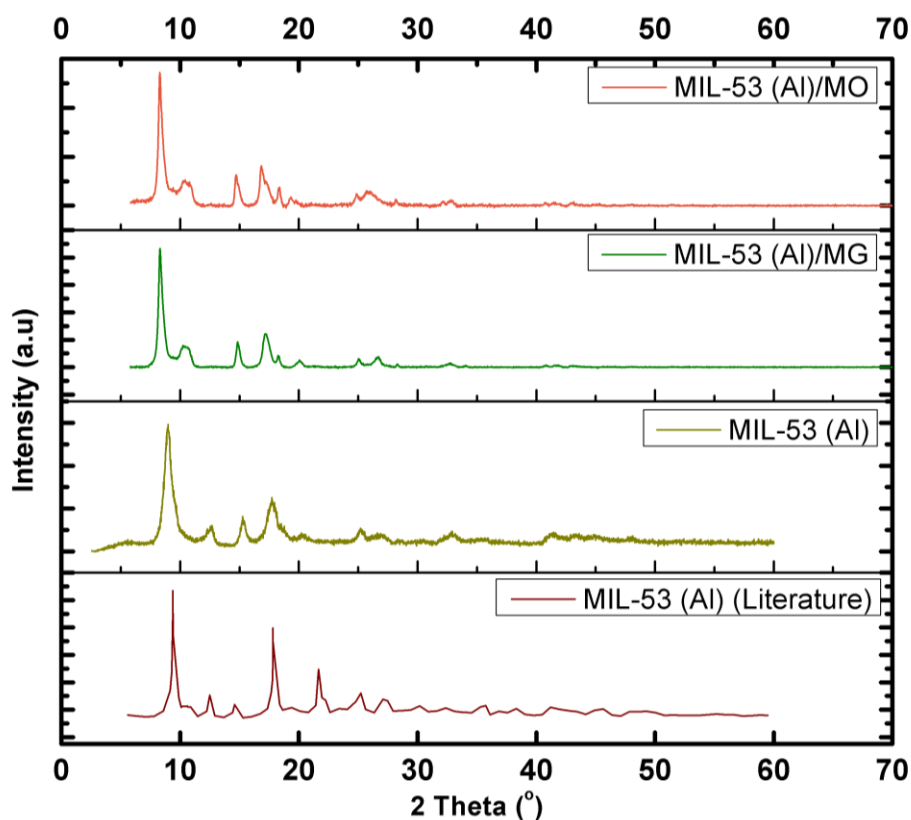


Figure 7: XRD patterns of MIL-53(Al) before and after MO and MG adsorption. Pattern from literature reported by Li et al. [70].

FT-IR spectra of MIL-53(Al) before and after the adsorption process are demonstrated in Figure 8. It can be seen that the obtained results are similar to those previously reported in the literature [93], [94]. The absorbance peak at 3495 cm^{-1} is assigned to -OH stretching vibration of adsorbed water on the surface [70]. Water molecules are present in MIL-53(Al) sample prior to adsorption due to the fact that this MOF absorbs some moisture from the air. However, after adsorption, the peak is still present due to the adsorption of water molecules from the prepared dye solution. The peak at 1690 cm^{-1} corresponds to -C=O stretching vibration [70]. The appearance of the peaks at 1596 and 1510 cm^{-1} is associated with the dissymmetry stretching vibration $\nu_{\text{asym}}(\text{CO}_2^-)$ of -(O-C-O)- [70]. On the other hand, symmetry stretching vibration $\nu_{\text{sym}}(\text{CO}_2^-)$ of -(O-C-O)- explains the peaks present at 1510 and 1416 cm^{-1} . The presence of peaks between 1260 to 965 cm^{-1} is because of the aromatic C-H in-plane bending, while aromatic C-H out of plane bending explains the peaks about 900 - 650 cm^{-1} . After the adsorption process of both MG and MO dyes, the intensity of the peaks was less and that corresponds to the interactions that might be present

between the functional groups in MIL-53(Al) and both dyes. Moreover, appearance of a new adsorption peak at 1150 cm^{-1} after adsorption of MG can be attributed to the presence of MG on the surface of the MOF. Also, the increase in intensity of the peak at 1750 cm^{-1} can be assigned to carboxylic stretching and the ligand-Al bond vibration. After adsorption of MO, a decrease in intensity in some of the peaks in the range of 450 to 1650 cm^{-1} is related to the hydrogen bond interaction between the OH group and MO.

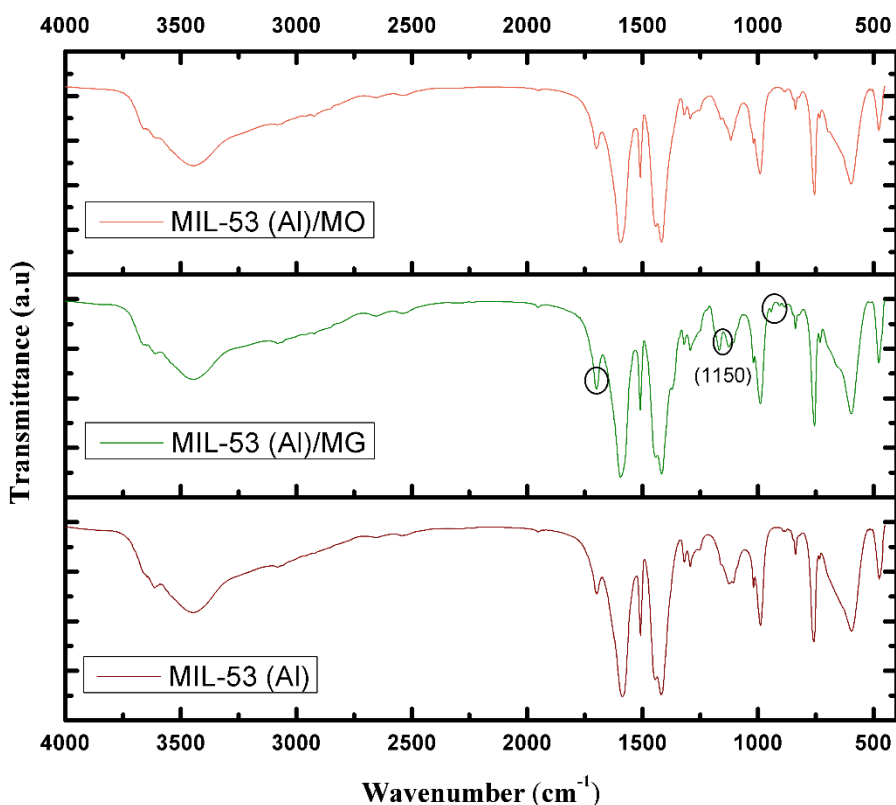


Figure 8: FT-IR spectra of MIL-53(Al) before and after MO and MG adsorption.

4.2. Removal Efficiencies

A comparison of the removal efficiency of MIL-53(Al) for both dyes in single-dye solution and binary-dye solution as a function of time is represented in Figure 9.

The removal efficiency of MO reached up to 99.5% within the first 10 minutes whereas, it reached 88.9% when MG was introduced as a competing solute as shown in Figure 9a. Similarly, it was observed that MIL-53 behaved better in removing MG as a single solute opposing to binary mixture of MO and MG as shown in Figure 9b. It can be seen that in 30 min, MG was completely removed in the single-dye solution,

while when being mixed with MO, the adsorption took 180 min to remove most of the dye (98.5%).

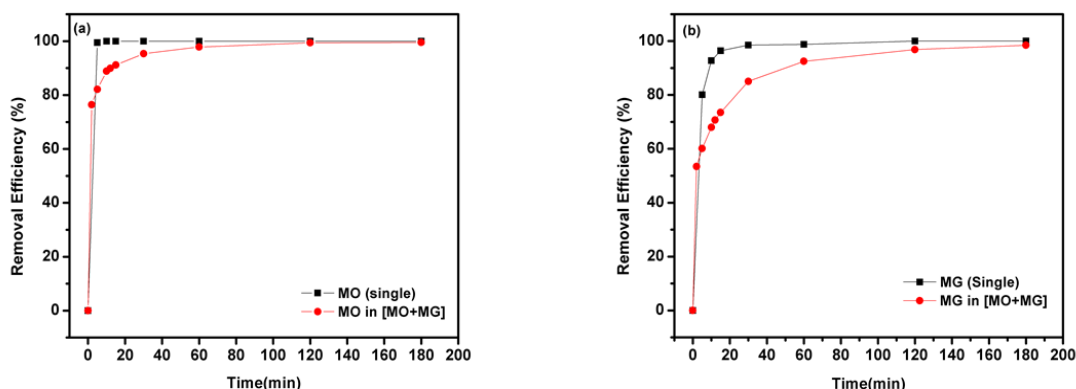


Figure 9: Comparison of (a) MO removal efficiency and (b) MG removal efficiency onto MIL-53(Al) in single and binary-dye solutions.

A comparison between the percentage removals of each dye suggests that the removal of MO was always greater than that of MG in both single and binary-dye solutions. This indicates that MIL-53(Al) has a higher affinity for MO than for MG. In addition, a competitive behavior between MO and MG explains the lower removal efficiencies of MO and MG in binary-dye solution than those in single-dye solution.

4.3. Point of Zero Charge and Effect of pH

The dye solution's initial pH is one of the significant factors that affect the adsorption process, precisely the adsorption capacity. The effect of pH on the adsorption capacity was examined up to an initial pH value of 10 since MG dye hydrolyzes in basic solution [70]. In this study, the adsorption capacities of MG and MO on MIL-53(Al) were determined at room temperature (25°C) after reaching equilibrium (60 min). The range of initial pH used to perform the adsorption experiments was 2-10. The dye solutions had an initial concentration of 7 mg L⁻¹ and the amount of adsorbent added was 10 mg of MIL-53(Al). Figure 10a demonstrates the effect of pH on MG and MO adsorption. When pH values were increased from 2 to 6, the adsorption capacity of both MG and MO increased as a result. It can be seen that MG and MO had the maximum adsorption capacities of 39.03 and 43.18 mg L⁻¹, respectively at a pH value of 6, which is the natural pH of both dyes. On the other hand, the adsorption capacities of both dyes decreased at pH ≥ 8. This could be due to the breakdown of MIL-53(Al) structure in alkaline solution [77].

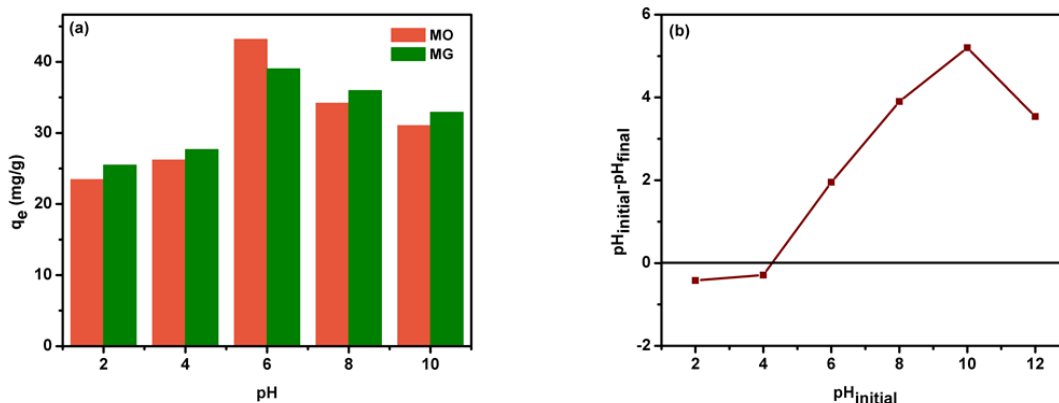


Figure 10: (a) Effect of solution pH on the adsorbed amount of MO and MG over MIL-53(Al); (b) Determination of MIL-53(Al) point of zero charge by plotting ΔpH vs. initial pH.

In order to understand and explain the effect of pH on the adsorption performance of MIL-53, point of zero charge (pH_{PZC}) plot was constructed as shown in Figure 10b. Accordingly, the pH_{PZC} was found to be at 4.4 pH. When pH is less than pH_{PZC} (4.4), the charge of the surface of the MOF is positive. This should contribute to the adsorption of the anionic dye MO, which is negatively charged on MIL-53(Al) by electrostatic interaction. However, the adsorption capacity of this dye on the adsorbent was found to be relatively low as given by the experimental data, which may suggest that the adsorption capacity of MIL-53(Al) to MO was not mainly controlled by the electrostatic interaction. The fact that the adsorption capacity increased when the pH of solution increased from 2 to 4 suggests that some other mechanism can be controlling the adsorption like hydrogen bond interaction or π - π stacking interactions. On the other hand, since MG is a cationic dye that is positively charged, less amounts of this dye will be adsorbed due to the electrostatic repulsion between MG and the adsorbent, which explains the experimental results and can be seen in Figure 10a. When pH is higher than pH_{PZC} , the MOF will be negatively charged. This is the case when pH is equal to 6, 8, and 10 in Figure 10a. The adsorption capacities of both dyes are higher than those obtained in low pH solutions. The electrostatic interaction between the positively charged MG and the MOF clearly explains this phenomenon. However, in the case of the negatively charged anionic dye MO, which should become less adsorbed due to the electrostatic repulsion, an opposite behavior was observed. This can be due to the damage that has happened to

the structure of MIL-53(Al) in basic solution and the hydrolysis of MO in basic solution that may transform it into another compound. Therefore, the adsorption of MO and MG on MIL-53(Al) can be explained by the adsorption mechanisms of electrostatic, hydrogen bond and π - π stacking interactions between the dyes and the MOF.

4.4. Effect of Initial Concentration

The initial concentration of a dye is one of the parameters that have a significant influence on the amount of dye being adsorbed. The effect of initial concentration of MG and MO on the removal efficiency of MIL-53(Al) is shown in Figures 11 and 12, respectively.

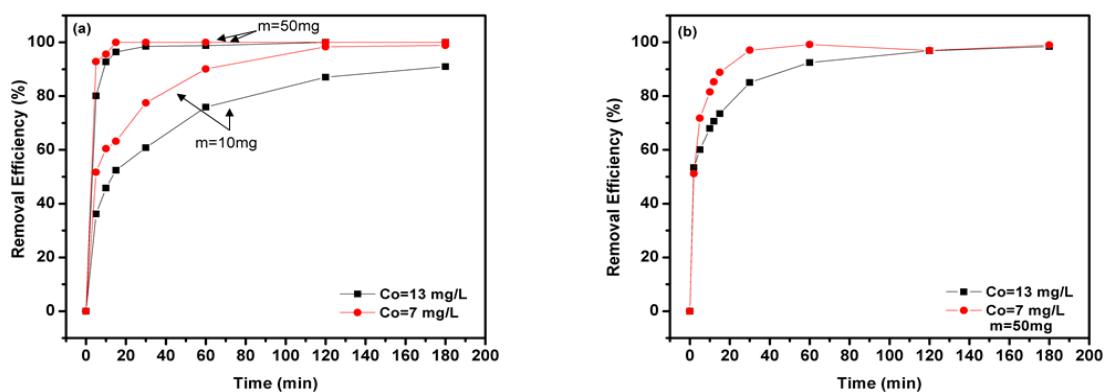


Figure 11 : Effect of initial concentration on the adsorbed amount of MG in (a) single-dye solution and (b) binary-dye solution.

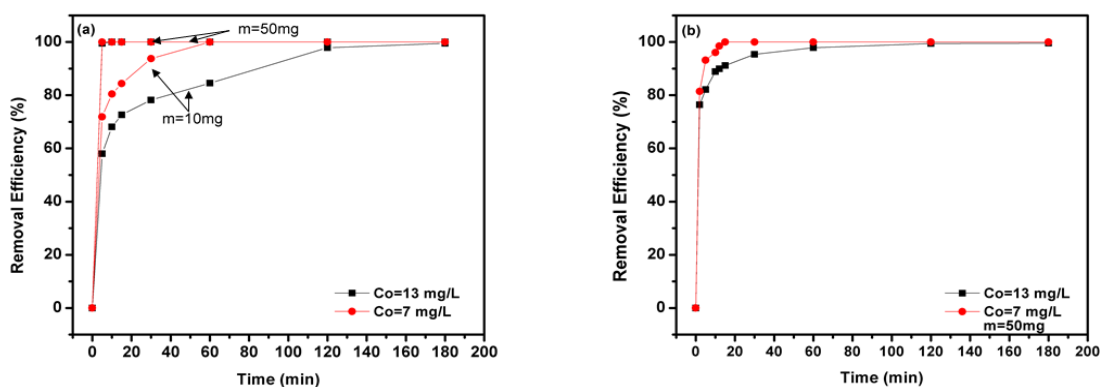


Figure 12: Effect of initial concentration on the adsorbed amount of MO in (a) single dye solution and (b) binary-dye solution.

The results demonstrated are obtained from both single and binary-dye solutions. It can be seen that an increase in MG initial concentration from 7 mg/L to

13 mg/L at a fixed amount of 50 mg or 10 mg of MOF leads to a decrease in the percentage removal of that dye in both single and binary solutions during a period of 3h. This finding can be attributed to the saturation of the available adsorption sites on the MOFs surface. However, the adsorption capacity of the MOF will increase as a result of increasing the initial concentration of the dye. This is because of the mass transfer between the dye and MOF, which require higher driving force at higher initial concentration of the dye [77]. In addition to that, adsorption capacity is defined as the amount of adsorbate (mg) per amount of adsorbent (g) (mg/g) which will be higher as the initial concentration of the dye increases per the same amount of adsorbent. On the other hand, two behaviors were noticed for the adsorption of MO in the single-dye solution. It remained intact with the increase of MO initial concentration when 50 mg of MOF was added, as 100% removal efficiency was achieved in 5 minutes at both concentrations, while when a dosage of 10 mg was used, a similar behavior to that obtained with MG was shown, as an increase in MO initial concentration led to a decrease in the percentage removal. The concentration-independent adsorption was not the case when studying the removal of MO from the binary solution as it had a similar behavior to that of MG when 50 mg of MOF was used.

4.5. Effect of Amount of MOF

Another factor that affects the adsorption process is the dosage of the adsorbent being added to the dye solution. Figures 13 and 14 and show the effect of MOF dosage on its removal efficiency of MO and MG dyes, respectively.

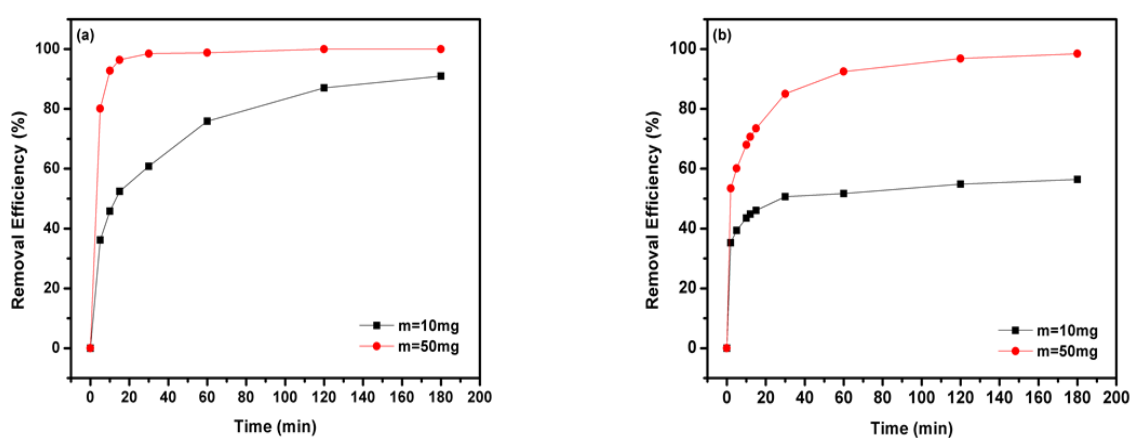


Figure13 : Effect of MIL-53(Al) dosage on the adsorbed amount of MG in (a) single dye solution and (b) binary-dye solution at an initial concentration of 13 mg/L.

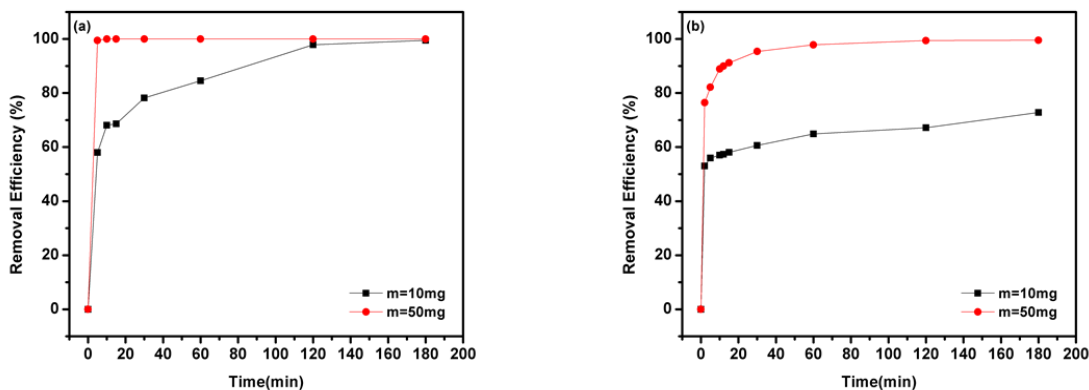


Figure 14: Effect of MIL-53(Al) dosage on the adsorbed amount of MO in (a) single dye solution and (b) binary-dye solution at an initial concentration of 13 mg/L.

The initial dye concentration was fixed at 13 mg/L in which an amount of 10 or 50 mg of MIL-53(Al) was added to carry out the experiments at room temperature. It can be seen that the percentage removal of both dyes whether in a single or a binary-dye solution when using an amount of 50 mg of MOF was higher than that when 10 mg of MOF was used during a period of 3h. This indicates that the higher the amount of MOF added, the higher the percentage of dye removal. This can be explained based on the fact that more MOFs mean more active sites available for adsorption hence increasing the amount of dye adsorbed [13]. This also explains the decrease in the adsorption capacity when increasing the MOF dosage.

4.6. Adsorption Kinetics

Four kinetic models were used to relate the experimental kinetic data for MG and MO dyes, these are, PFO, PSO, Elovich, and Intraparticle Diffusion models. The kinetic parameters and R^2 values for MO and MG adsorption are presented in Table 7 and 8, respectively. It can be seen that MG adsorption over MIL-53(Al) follows a PSO model, whether it was present in a single or binary-dye solution. On the other hand, the adsorption of MO in a single dye solution followed both PFO and PSO models, while the PSO model provided the best fit for the data in the case of a binary-dye solution. Therefore, it can be proposed that MG and MO adsorption are most likely controlled by chemisorption as the rate-limiting step [18]. Moreover, Figure 15 demonstrates the plots of q_t versus t obtained from the PSO model for both MO and MG dyes in single and binary solutions.

Table 7: Kinetic parameters for MO adsorption in single and binary-dye solutions

| Type of MO Solution | Kinetic Model | Kinetic Parameters | Initial Concentration, C ₀ (mg/L) | | |
|--|-----------------------------|--|--|-------------------------|--------|
| | | | 7 | 13 | |
| Single Dye Solution | PFO | q _e (exp) (mg.g ⁻¹) | 5.551 | 8.153 | |
| | | k ₁ (min ⁻¹) | 2.352 | 8.962 | |
| | | q _e (cal) (mg.g ⁻¹) | 5.551 | 8.146 | |
| | PSO | R ² | 1.000 | 1.000 | |
| | | k ₂ (g.mg ⁻¹ .min ⁻¹) | 5.834 | 4.886 | |
| | | q _e (cal) (mg.g ⁻¹) | 5.551 | 8.159 | |
| | Elovich | R ² | 1.000 | 1.000 | |
| | | α(mg.g ⁻¹ .min ⁻¹) × 10 ¹⁰ | 1.611 | 4.934 | |
| | | β(g.mg ⁻¹) | 5.160 | 3.609 | |
| | Binary-Dye Solution [MG+MO] | PFO | R ² | 0.985 | 0.987 |
| | | | q _e (exp) (mg.g ⁻¹) | 7.015 | 12.899 |
| | | | k ₁ (min ⁻¹) | 0.847 | 0.786 |
| q _e (cal) (mg.g ⁻¹) | | | 6.926 | 12.120 | |
| PSO | | R ² | 0.996 | 0.971 | |
| | | k ₂ (g.mg ⁻¹ .min ⁻¹) | 0.301 | 0.118 | |
| | | q _e (cal) (mg.g ⁻¹) | 7.103 | 12.620 | |
| Elovich | | R ² | 0.999 | 0.996 | |
| | | α(mg.g ⁻¹ .min ⁻¹) | 1.587 × 10 ¹⁰ | 1.265 × 10 ⁶ | |
| | | β(g.mg ⁻¹) | 4.124 | 1.479 | |
| | | R ² | 0.986 | 0.993 | |

Table 8: Kinetic parameters for MG adsorption in single and binary solutions

| Type of MG Solution | Kinetic Model | Kinetic Parameters | Initial Concentration, C ₀ (mg/L) | |
|-----------------------------|---------------|---|--|-----------------------|
| | | | 7 | 13 |
| | | q _e (exp) (mg.g ⁻¹) | 7.892 | 14.397 |
| Single Dye Solution | PFO | k ₁ (min ⁻¹) | 0.530 | 0.324 |
| | | q _e (cal) (mg.g ⁻¹) | 7.848 | 14.200 |
| | | R ² | 0.998 | 0.998 |
| | PSO | k ₂ (g.mg ⁻¹ .min ⁻¹) | 0.299 | 0.057 |
| | | q _e (cal) (mg.g ⁻¹) | 7.958 | 14.640 |
| | | R ² | 0.999 | 0.999 |
| | Elovich | α(mg.g ⁻¹ .min ⁻¹) | 3.674×10 ¹⁰ | 4.247×10 ⁷ |
| | | β(g.mg ⁻¹) | 3.751 | 1.565 |
| | | R ² | 0.994 | 0.988 |
| Binary-Dye Solution [MG+MO] | PFO | q _e (exp) (mg.g ⁻¹) | 6.992 | 13.157 |
| | | k ₁ (min ⁻¹) | 0.309 | 0.257 |
| | | q _e (cal) (mg.g ⁻¹) | 6.640 | 11.550 |
| | | R ² | 0.970 | 0.861 |
| | PSO | k ₂ (g.mg ⁻¹ .min ⁻¹) | 0.0704 | 0.0145 |
| | | q _e (cal) (mg.g ⁻¹) | 7.104 | 13.450 |
| | | R ² | 0.997 | 0.999 |
| | Elovich | α(mg.g ⁻¹ .min ⁻¹) | 221.5 | 83.460 |
| | | β(g.mg ⁻¹) | 1.455 | 0.681 |
| | | R ² | 0.956 | 0.995 |

When using the PSO model, the calculated values of q_e are similar to the experimental values for both dyes, whether in a single or binary dye solution. The PSO rate constant (k₂) was found to decrease when increasing the initial concentration of MO and MG dyes from 7 to 13 mg/L. This can be due to the increase in the competition for available sites on the surface of the MOF [74], [75]. Moreover, the rate constants for MO adsorption were higher than the ones obtained for MG adsorption, agreeing with the greater removal efficiency of MIL-53(Al) for MO dye.

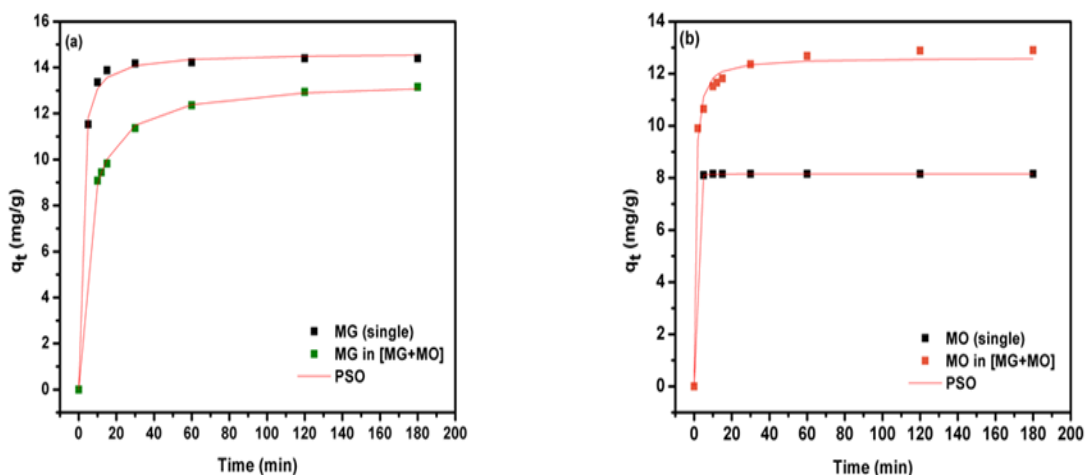


Figure 15: PSO models for the removal of (a) MG and (b) MO in single and binary solutions at an initial concentration of 13 mg/L and 50 mg of MOF.

Figure 16 shows the results of the intraparticle diffusion study on MO and MG dyes in both single and binary-dye solutions. For the used concentrations of 7 and 13 mg/L, the range of the correlation coefficients (R^2) was 0.94 to 0.98 and the constants (C_i) had positive values. This suggests that the External Diffusion Model should be used to fit the experimental data. It can be seen from Figure 16 that the linear segments of plots do not pass through the origin, implying that the adsorption process of MO and MG dyes onto MIL-53(Al) includes several stages and that intraparticle diffusion is not the rate controlling step. Such behavior was investigated in previous studies on adsorption [95], [96].

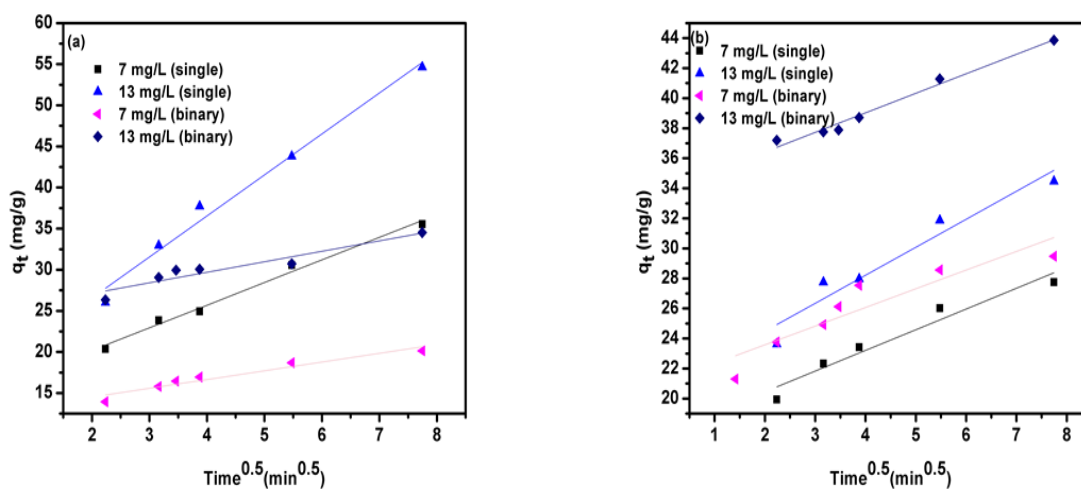


Figure 16: Intraparticle Diffusion model for the removal of (a) MG and (b) MO in single and binary solutions with 50 mg of MOF.

4.7. Adsorption Isotherms

The nonlinear fittings of Freundlich isotherm of MG and MO in single dye solution at 25° with 10 mg of MOF are plotted in Figure 17.

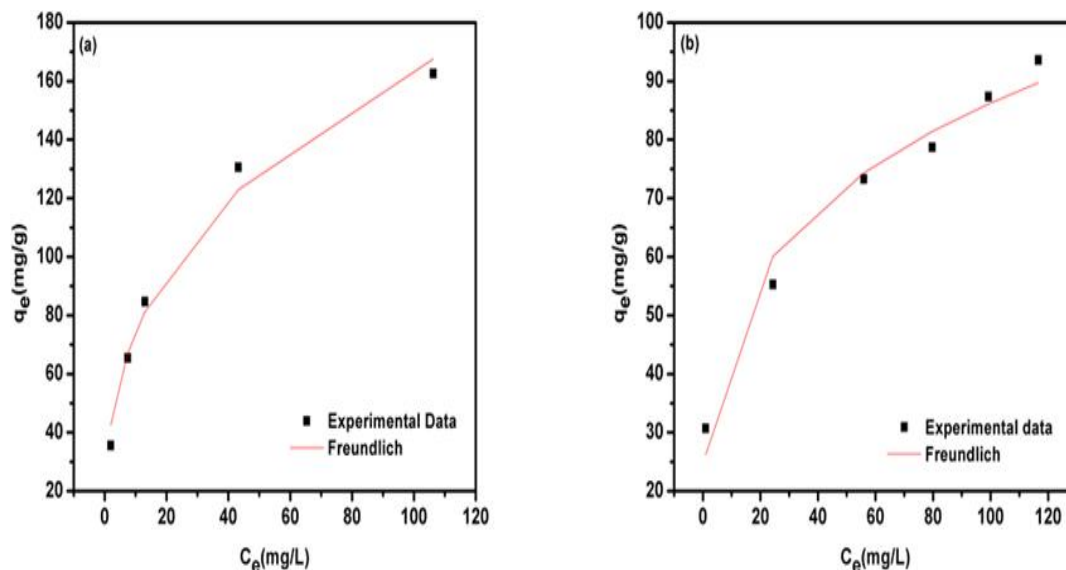


Figure 17: Freundlich model for the removal of (a) MG and (b) MO in single dye solutions with 10 mg of MOF at 298 K.

As can be seen from the plots, increasing the initial concentrations of both dyes results in a considerable increase in the adsorption capacities. A similar behavior was observed at all other temperatures of 35, 45 and 65°C at a range of initial concentration up to 120 mg/L. This can be attributed to the enhancement of collision between the dyes and the MOF caused by the increase of the initial concentration.

The isotherm parameters computed according to Langmuir and Freundlich models together with the R^2 values are provided in Table 10. This table indicates that the data are best fitted using the Freundlich isotherm model for both MG and MO. This implies that the adsorption of MG and MO into MIL-53(Al) is controlled by a multilayer adsorption [97]. Hence, this model assumes both chemical and physical adsorption. n value was higher than 1 at all temperatures for both dyes, which indicates the favorability of the adsorption process, MIL-53(Al) has affinity to both anionic and cationic dyes [19], and that the adsorption is heterogeneous.

Table 9: Adsorption isotherm parameters of single dye adsorption by MIL-53(Al) at various temperatures

| Dyes | Isotherm Model | Isotherm Parameters | Temperature (K) | | | |
|------|------------------|---|-----------------|--------|--------|-------|
| | | | 298 | 308 | 318 | 338 |
| MO | Langmuir model | K_L (L.mg ⁻¹) | 0.078 | 0.128 | 0.138 | 0.224 |
| | | q_m (mg.g ⁻¹) | 176.6 | 182.5 | 208.3 | 219.4 |
| | | R^2 | 0.979 | 0.869 | 0.876 | 0.946 |
| | Freundlich model | K_F (mg.g ⁻¹)(L.mg ⁻¹) ^{1/n} | 33.520 | 47.200 | 60.360 | 67.62 |
| | | n | 2.899 | 3.408 | 3.845 | 3.858 |
| | | R^2 | 0.986 | 0.999 | 0.990 | 0.967 |
| MG | Langmuir model | K_L (L.mg ⁻¹) | 0.472 | 0.035 | 0.045 | 0.089 |
| | | q_m (mg.g ⁻¹) | 81.2 | 134.3 | 143.5 | 128.8 |
| | | R^2 | 0.745 | 0.660 | 0.815 | 0.929 |
| | Freundlich model | K_F (mg.g ⁻¹)(L.mg ⁻¹) ^{1/n} | 26.560 | 40.350 | 28.36 | 46.62 |
| | | n | 3.910 | 5.049 | 3.210 | 5.029 |
| | | R^2 | 0.974 | 0.900 | 0.900 | 0.986 |

4.8. Adsorption Thermodynamics

Based on the MG and MO adsorption isotherm data, the value of $\ln(K_{eq})$ at a specific temperature is calculated by graphing a plot of $\ln(q_e/C_e)$ against q_e and extrapolating q_e to zero [98]. Equation was used to compute the adsorption free energy change (ΔG°), while the change in enthalpy (ΔH°) and entropy (ΔS°) for MG and MO adsorption were derived from the Van't Hoff plot, shown in Figure 18. These obtained thermodynamics parameters are presented in Table 11. The negative values of the Gibbs free energy change (ΔG°) for both dyes suggest the spontaneous nature of the adsorption process. When increasing the temperature, the values of (ΔG°) decrease, which accounts for a drop in the probability of adsorption at greater temperatures. Furthermore, it can be seen that ΔG° values for MO are more negative than those of MG, suggesting more favorability to the adsorption of MO onto MIL-53(Al) [87], which is in good agreement with the obtained results. According to literature, if ΔG° is between -20-0 kJ/mol, the adsorption is physical, whereas it is considered chemical if it is between -400 to -80 kJ/mol. The range of ΔG° values in

this study indicate that the adsorption is not a solely chemical or physical adsorption, but a little bit of both [70]. Positive values of the change in enthalpy (ΔH°) were found for the adsorption of both dyes on MIL-53(Al). This indicates that the adsorption process is endothermic. The entropy change (ΔS°) was also found to be positive for both dyes, which suggests that the randomness of the dye at the MOF-solution interface increased. This happened because the water molecules were desorbed from the surface of the MOF [99].

Table 10 : Thermodynamic parameters of MO and MG adsorption by MIL-53(Al)

| Dyes | ΔG° (kJ.mol ⁻¹) | | | | ΔH° (kJ.mol ⁻¹) | ΔS° (J.mol ⁻¹ .K ⁻¹) |
|------|--|--------|--------|--------|--|--|
| | 298 K | 308 K | 318 K | 338 K | | |
| MO | -35.35 | -37.81 | -39.25 | -43.08 | 22.18 | 193.11 |
| MG | -34.55 | -37.21 | -36.02 | -40.16 | 27.22 | 199.24 |

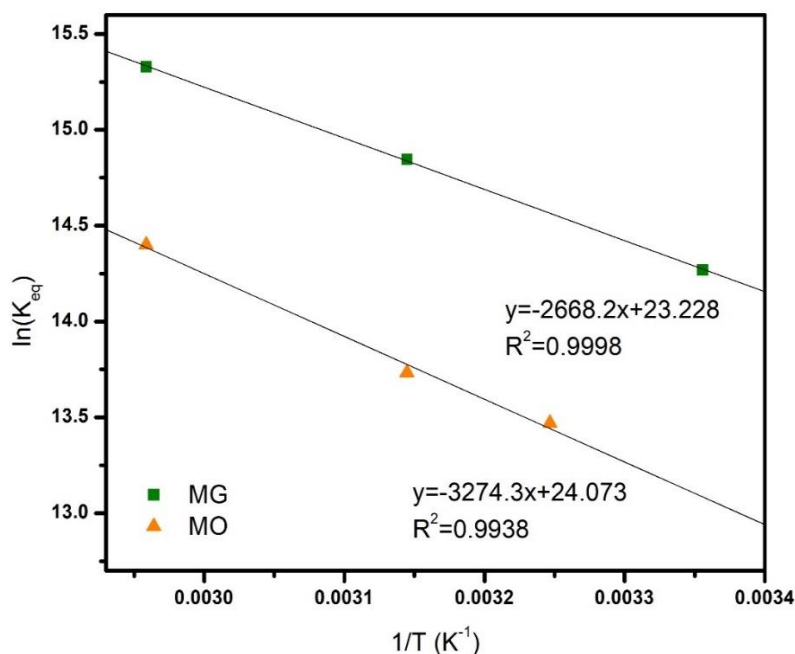


Figure 18: Van't Hoff plot for ΔH° and ΔS° measurement of MO and MG adsorption on MIL-53(Al).

4.9. Selectivity of Binary-Dye Adsorption

Table 11 shows the adsorption selectivity for binary-dye solutions at initial concentrations of 7 and 13 mg.L⁻¹ with addition of 10 or 50 mg of MIL-53(Al). The selectivity was calculated using Equation (13) by choosing Methyl Orange as dye 1 and Malachite Green as dye 2. The selectivity was always higher than 1, which indicates that MIL-53(Al) has a higher affinity for MO than for MG. Figure 18 represents the effect of initial concentration on the selectivity at fixed amounts of MOF. It can be seen from the figure that the selectivity decreases with the increase of the initial concentration of the dyes at a fixed amount of MOF. This finding can be attributed to the saturation of the available adsorption sites on the MOF's surface. On the other hand, increasing the amount of MOF added to the solution results in increasing the selectivity at a fixed initial concentration. This is due to the fact that more active sites are available for adsorption hence increasing the adsorbed amount of the favorable dye (MO). These results agree with the high removal efficiencies at lower initial concentrations and higher amount of dosage. Therefore, selective adsorption of MO is favorable at these operating conditions.

Table 11: Selectivity at different initial concentrations and MOF dosage

| MOF Dosage (mg) | Initial Concentration, (mg.L ⁻¹) | |
|-----------------|--|-------|
| | 7 | 13 |
| 10 | 4.438 | 2.067 |
| 50 | 13.582 | 3.412 |

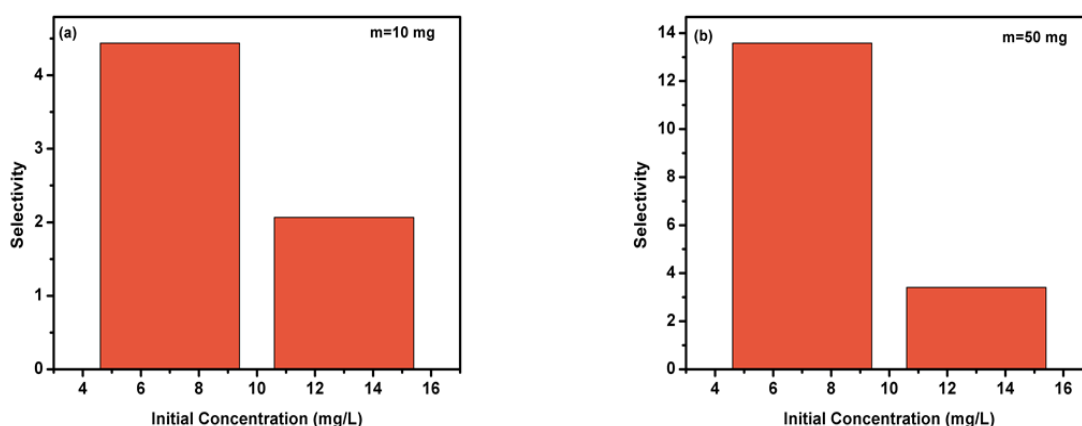


Figure 19: Adsorption selectivity for binary-dye solutions at initial concentrations of 7 and 13 mg. L⁻¹ with addition of (a) 10 and (b) 50 mg of MIL-53(Al).

4.10. Regeneration of MIL-53(Al)

The ability to regenerate and reuse adsorbents can help in cost and dosage reduction when removing pollutants from wastewater in industrial processes, as they will be used for extended amount of time. To investigate the endurance of MIL-53(Al) over the long term, its reusability was examined in the binary-dye adsorption process. First, a MOF dosage of 50 mg was activated by washing it with 70% ethanol for 3h. Then, it was used for the removal of MO and MG in a binary-dye solution of an initial concentration of 13 mg/L. After the adsorption process, centrifugation was used to split up MIL-53(Al) particles from the liquid solution (4000 rpm for 2 min). Then, 70% ethanol was used to wash MIL-53(Al) from the adsorbed dyes. Finally, using an oven, the MOF was dried at 100° C and used for the next experiment.

Figure 19 represents the influence of the regeneration cycles on the adsorption capacity of MO and MG into MIL-53(Al). It can be seen that the adsorption capacity stayed intact as the recycle times increased, suggesting that this washing method for removing MO and MG dyes was a success.

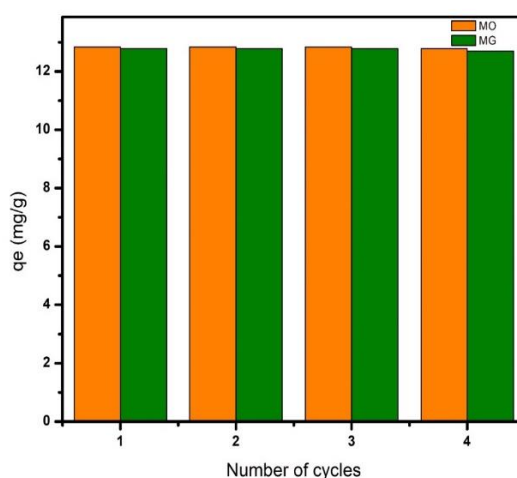


Figure 20: Effect of number of cycles of MIL-53(Al) on MG and MO binary adsorption at 298 K, $C_o = 13$ mg/L, and $m=50$ mg.

4.11. Factorial Design

The three experimental factors that were used to create the full factorial design were the dosage of MIL-53(Al), the initial concentration of MG, and the initial concentration of MO. A study on the effect of these factors on the adsorption capacity of MIL-53(Al) in binary-dye solutions of MO and MG was carried out in accordance to the design matrix. Each factor has two levels encrypted as +1 for high level, and -1

for low level, which are presented in Table 12. A total of 16 runs were performed with random order to dodge any systematic error that might occur. Table 13 lists the design matrix that was used to carry out these runs. The results were analyzed by employing factorial plots: pareto chart, main effects plot, and interaction plot. Figure 21 represents the cube plot which demonstrates the means of the response for the levels of the variables used in the design.

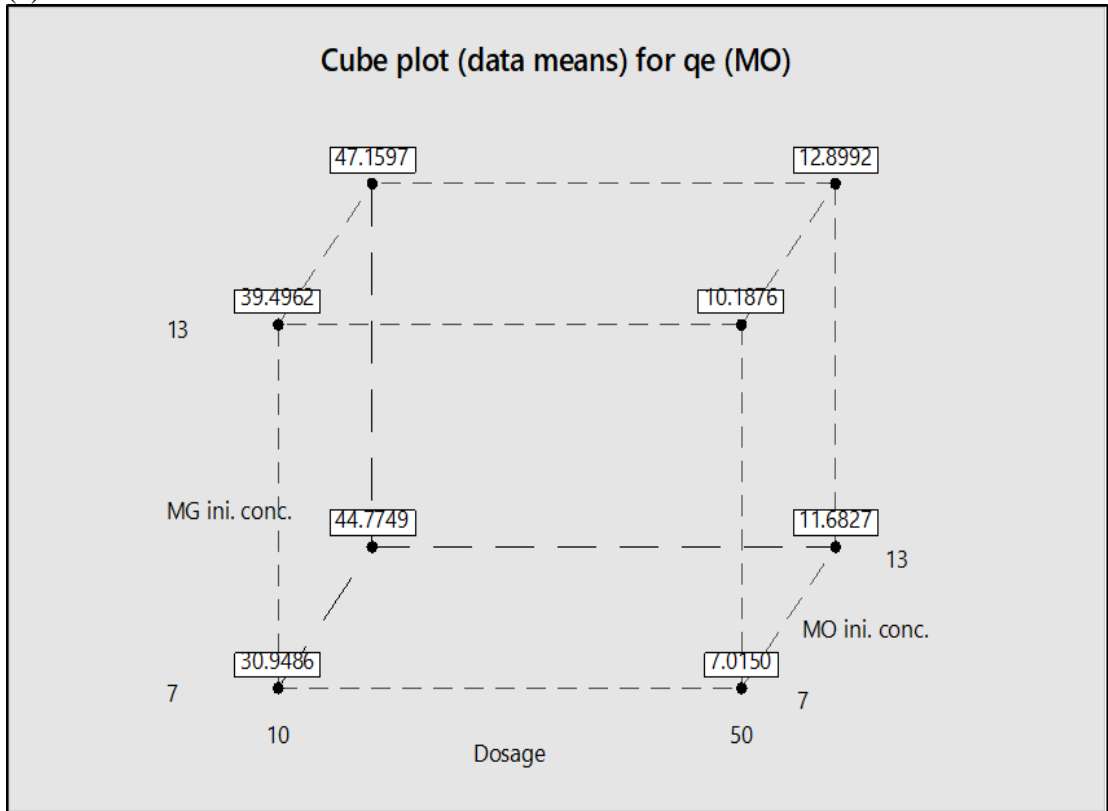
Table 12: The factorial design's factors and levels

| Factor | Symbol | Low Level (-1) | High Level (+1) |
|--|---------------|-----------------------|------------------------|
| Dosage (mg) | A | 10 | 50 |
| MG initial concentration (mg/L) | B | 7 | 13 |
| MO initial concentration (mg/L) | C | 7 | 13 |

Table 13: Design matrix and results for MG and MO adsorption capacity

| Run | A | B | C | q_e (MG), (mg/g) | q_e (MO), (mg/g) |
|------------|----------|----------|----------|-----------------------------------|-----------------------------------|
| 1 | 50 | 7 | 7 | 7.089 | 6.978 |
| 2 | 10 | 13 | 13 | 40.058 | 49.679 |
| 3 | 10 | 13 | 13 | 35.322 | 44.641 |
| 4 | 50 | 13 | 13 | 13.112 | 12.840 |
| 5 | 50 | 13 | 7 | 12.955 | 10.118 |
| 6 | 10 | 7 | 13 | 22.948 | 43.944 |
| 7 | 50 | 7 | 13 | 7.058 | 11.726 |
| 8 | 50 | 7 | 7 | 6.894 | 7.053 |
| 9 | 10 | 13 | 7 | 34.280 | 38.799 |
| 10 | 50 | 13 | 7 | 13.314 | 10.257 |
| 11 | 50 | 13 | 13 | 13.201 | 12.958 |
| 12 | 50 | 7 | 13 | 6.869 | 11.640 |
| 13 | 10 | 7 | 7 | 22.286 | 31.083 |
| 14 | 10 | 7 | 13 | 23.359 | 45.606 |
| 15 | 10 | 7 | 7 | 22.096 | 30.815 |
| 16 | 10 | 13 | 7 | 31.692 | 40.193 |

(a)



(b)

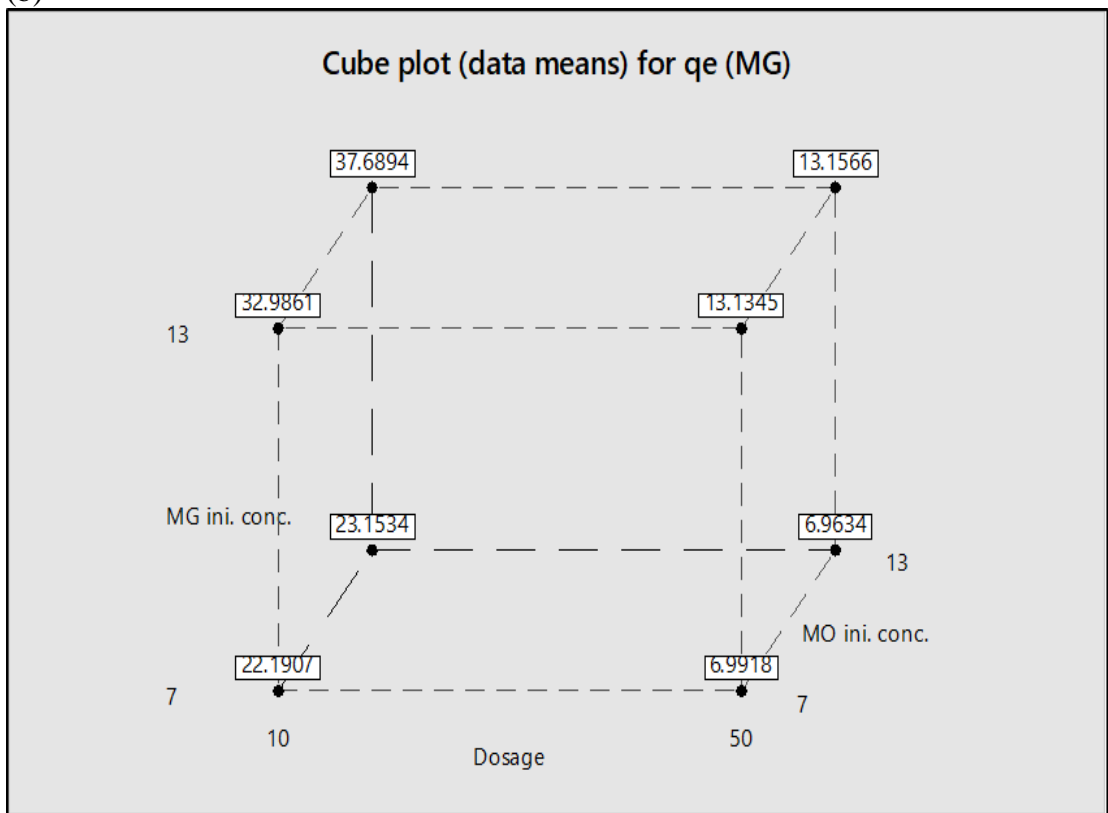


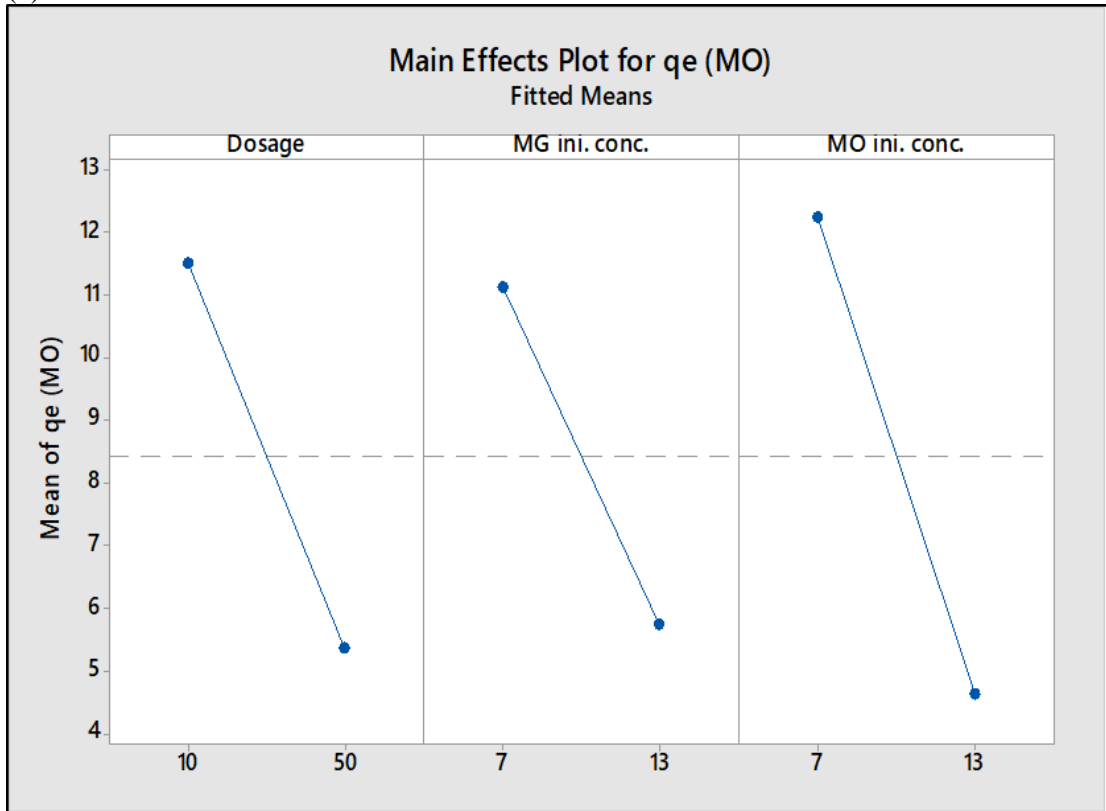
Figure 21: Cube plot for adsorption capacity of (a) MO and (b) MG removal.

Table 14 lists the 2³ factorial designs' main effect, 2-way and 3-way interaction effects, coefficients of the model and their standard deviation, and probability. A t-test was used to indicate the importance of the regression coefficients with 95% confidence level. It can be seen that all MO effects were important except for the 3-way interaction (ABC), while in MG, A, B, and AB were the factors that were considered significant. The absolute value of the effect is what indicates the significance of the factors being considered. Moreover, an adjusted square correlation coefficient R² of 99.21% for MG and 99.62% for MO was displayed by the model.

Table 14: Estimated effects and coefficients for adsorption capacity of MIL-53(Al) for both dyes

| Term | Effect | Coef | SE Coef | T-Value | P-Value |
|-------------|---------------|-------------|----------------|----------------|----------------|
| MG | | | | | |
| Constant | | 19.533 | 0.340 | 57.51 | 0.000 |
| A | -18.943 | -9.472 | 0.340 | -27.89 | 0.000 |
| B | 9.417 | 4.708 | 0.340 | 13.86 | 0.000 |
| C | 1.415 | 0.707 | 0.340 | 2.08 | 0.071 |
| AB | -3.249 | -1.624 | 0.340 | -4.78 | 0.001 |
| AC | -1.418 | -0.709 | 0.340 | -2.09 | 0.070 |
| BC | 0.948 | 0.474 | 0.340 | 1.40 | 0.200 |
| ABC | -0.923 | -0.461 | 0.340 | -1.36 | 0.212 |
| MO | | | | | |
| Constant | | 25.520 | 0.343 | 74.31 | 0.000 |
| A | -30.149 | -15.074 | 0.343 | -43.89 | 0.000 |
| B | 3.830 | 1.915 | 0.343 | 5.58 | 0.001 |
| C | 7.217 | 3.609 | 0.343 | 10.51 | 0.000 |
| AB | -1.636 | -0.818 | 0.343 | -2.38 | 0.044 |
| AC | -3.528 | -1.764 | 0.343 | -5.14 | 0.001 |
| BC | -2.030 | -1.015 | 0.343 | -2.95 | 0.018 |
| ABC | 1.052 | 0.526 | 0.343 | 1.53 | 0.164 |

(a)



(b)

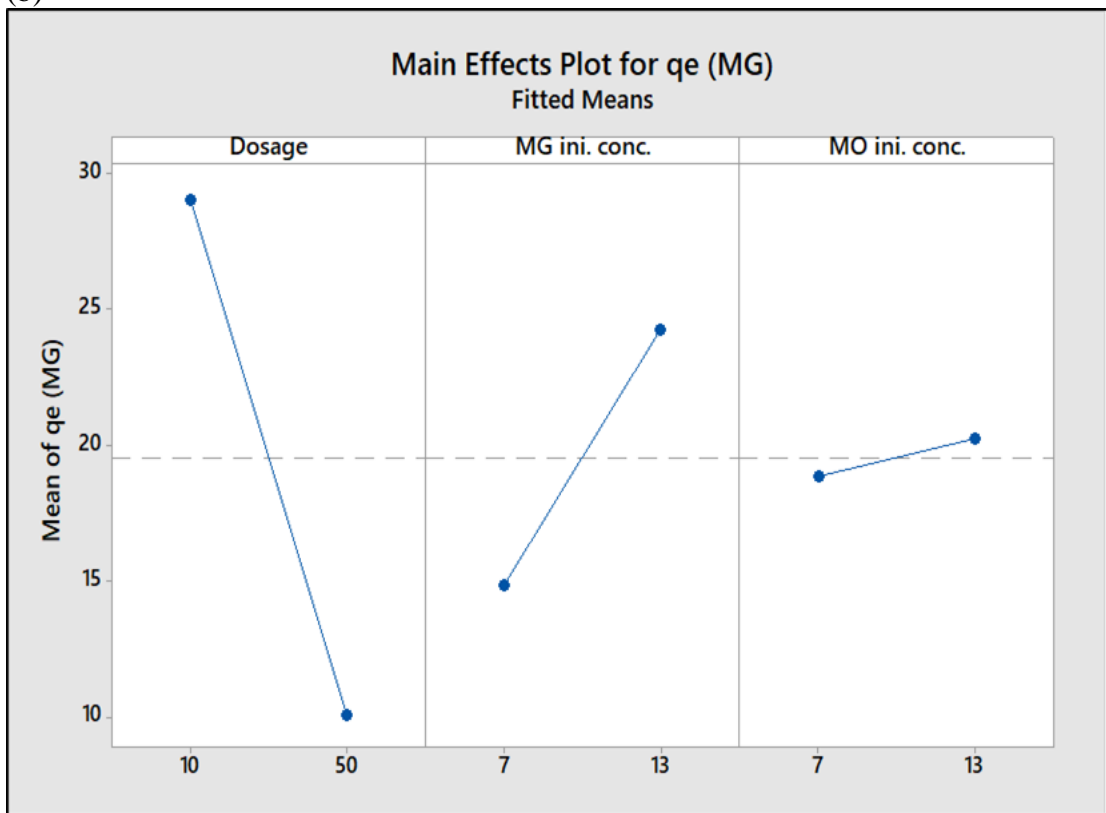


Figure 22: Main effects plot for adsorption capacity of (a) MO and (b) MG removal.

Equations (14) and (15) were used to relate the adsorption capacity for the removal of the two dyes with the process factors in coded terms as follows:

$$qe (MO) = -3.23 - 0.031 A + 3.051 B + 4.089 C - 0.0428 AB - 0.0586 AC - 0.2004 BC + 0.00292 ABC \quad (14)$$

$$qe (MG) = 16.97 - 0.341 A + 1.086 B - 0.705 C - 0.0014 AB + 0.0138 AC + 0.1295 BC - 0.00256 ABC \quad (15)$$

These equations depict the effect the experimental factors and their interactions have on the adsorption process of the dyes. The coefficients used in these equations are provided in Table 14.

In order to study how the means and strengths of every process variable differ at various levels, the main effects plot was utilized as shown in Figure 22. Since there are no horizontal lines connecting the mean for each parameter's levels, there is a main effect for every variable. There was a negative influence on the adsorption capacity for the removal of both dyes due to the increase in the adsorbent dosage. In the case of MO removal, increasing the initial concentrations of either dye resulted in reversible effects, while for MG removal, the increment in the dyes initial concentration had positive effects on the adsorption capacity. Also, in case of MG removal, the initial concentration of MO had an insignificant effect on the adsorption capacity, which was not the case for MO removal in terms of MG initial concentration as the later had a significant effect on the adsorption process. These findings agree with the results acquired from the adsorption experiments.

Figure 23 presents the interaction effects of the experimental factors on the adsorption capacity for the removal of MO and MG. In case there is no parallelism between the lines, the interaction is considered strong among these factors and vice versa [100]. For MO adsorption, the interaction between the MOF dosage and each dye initial concentration as well as the interaction between the initial concentration of both dyes are considered important. It can be seen from the AB and AC graphs that changing the dosage of the MOF from 10 mg to 50 mg had a higher effect at a lower initial concentration of both dyes. Also, BC plot revealed that when increasing MG initial concentration, a lower MO initial concentration had the higher response. In case of MG adsorption, the interaction between the MOF dosage and MO initial

concentration along with the interaction between the initial concentration of each dye are considered of less importance since the lines are almost parallel. On the other hand, increasing the MOF dosage had a higher effect at a higher initial concentration of MG.

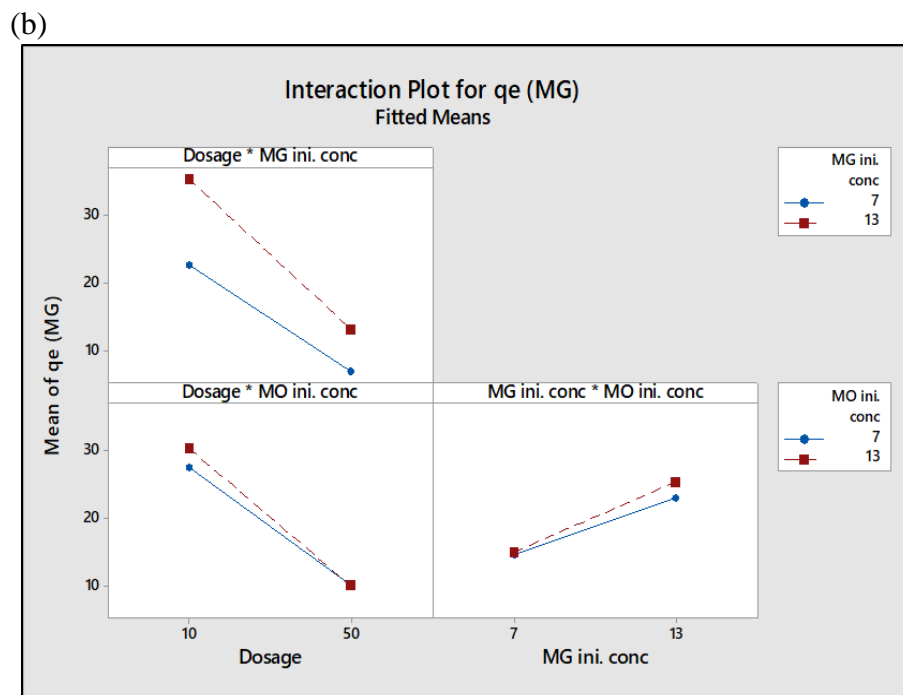
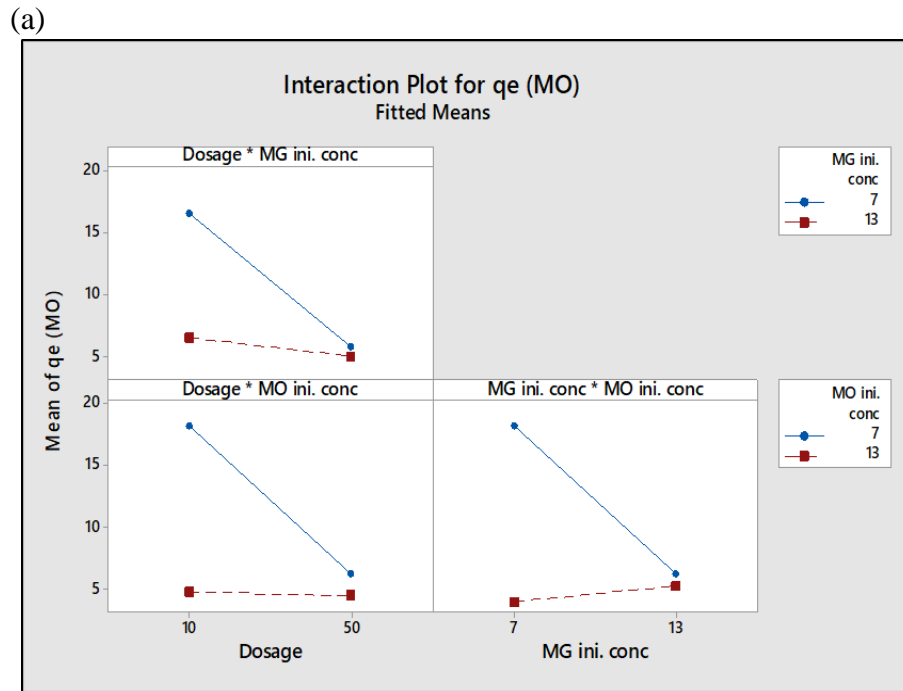
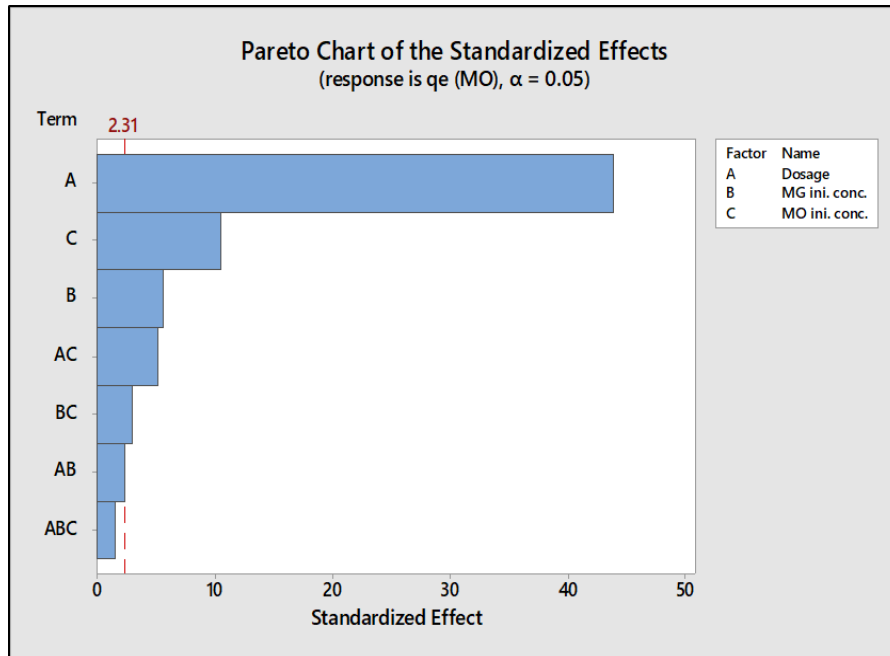


Figure 23: Interaction effects plot for adsorption capacity of (a) MO and (b) MG.

The Pareto chart also displays the relative significance of the main effects and the interactions as can be seen in Figure 24. It can be utilized to obtain the standardized effects and arrange them from the largest to the smallest [101].

(a)



(b)

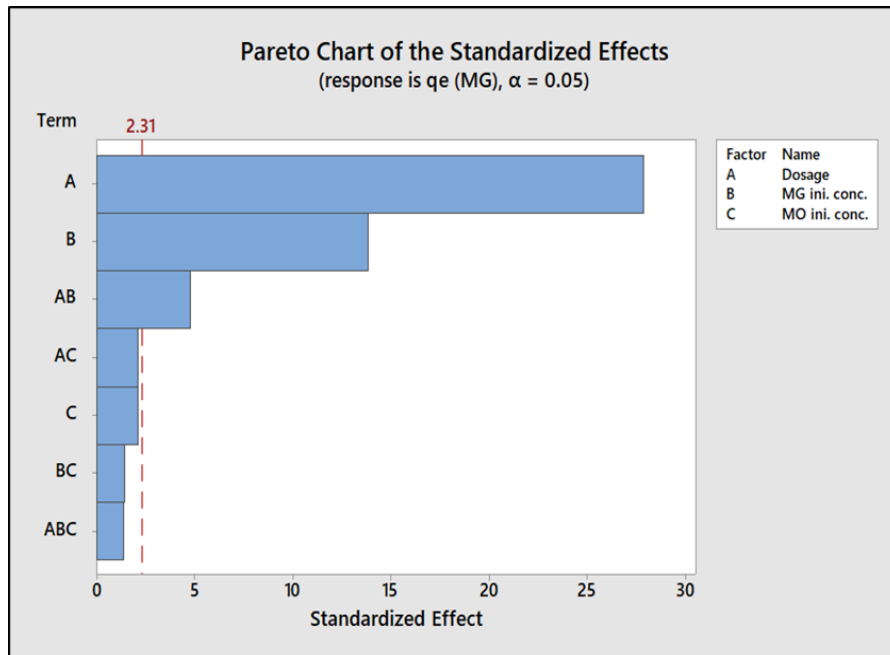


Figure 24: Pareto chart of the effects of (a) MO and (b) MG removal.

The variables that cross the reference line, which was found to be 2.31, are of high significance to the adsorption process and those that do not are insignificant. In case of MO adsorption, all factors are considered significant at the level of 0.05 except for the 3-way interaction ABC as it did not extend beyond 2.31. On the other hand, only A, B and their interaction were considered significant for MG removal.

Chapter 5. Conclusions and Future Work

Adsorptive removal of cationic and anionic dyes from aqueous solutions using Metal Organic Framework (MOF) was investigated in this thesis. Malachite Green (MG) and Methyl Orange (MO) were the dyes that were used as the model adsorbates, while MIL-53(Al) was the adsorbent of which performance was examined. Single and binary-dye solutions were prepared to carry out the batch adsorption experiments. Different factors were found to have an effect on the adsorption process such as MOF dosage, initial dye concentration, pH of the solution and temperature. In case of single-dye solutions, MO was completely removed from the solution within the first 5 minutes, while it took 15 minutes to remove MG at the optimum operating conditions. More time was needed to remove both dyes in binary-dye solutions at the same conditions due to the competitive behavior between MO and MG. MO was removed in 12 minutes, while 180 minutes were needed for MG to be completely adsorbed, indicating the selective adsorption of MO over MG. Pseudo-second order model was the model that the kinetics data followed with $R^2 > 0.996$ for both dyes. Isotherm data were best fitted to the Freundlich isotherm model for each of the dyes. The high adsorption behaviour of MIL-53(Al) is interpreted from hydrogen bonding and π - π stacking interactions between the dyes and the MOF surface. The adsorption of both kinds of dyes was found to be spontaneous and endothermic as indicated from the thermodynamics parameters (ΔG° , ΔH° , ΔS°). The selectivity test for an equimolar binary-dye solution containing both MG and MO suggested the higher affinity of MIL-53(Al) towards MO over MG, as it reached a value of 13.582 at an initial concentration of 7 mg/L and 50 mg of MOF. Regeneration of MIL-53(Al) was possible by washing it with 70% ethanol and reusing it for over 4 cycles of adsorption-desorption with almost no reduction in the adsorption capacity. Accordingly, this study shows that Al-based MOFs, especially MIL-53(Al), has the ability to become a promising candidate for the removal of a diversity of azo dyes.

For future work, it is recommended to use Scanning Electron Microscopy (SEM) to have a better understanding of the microstructure of the MOF and investigate its shape, size, and texture. Moreover, the thermal stability of MIL-53(Al) can be determined by using Thermal gravimetric Analysis (TGA) which can also identify its fraction of volatile elements. Another characterization test that would be

helpful in determining the surface area and the pore size of the powder material is the Brunauer–Emmett–Teller (BET), which should be investigated as well.

The future aim is to have more studies on the simultaneous adsorption of more than two kinds of dyes, whether anionic or cationic, as there is not enough information about this topic and comparing multiple adsorbates would provide a better understanding of the adsorption process. Furthermore, dyes can be present in wastewater along with other kinds of micropollutants such as pharmaceuticals, therefore; the removal of dyes from a multicomponent mixture should be investigated in order to have a better understanding of the adsorption process. Moreover, the continuous adsorption behaviour of MIL-53(Al) in a fixed-bed should be evaluated for both single and binary-dye solutions for industrial and commercial scale use. Also, more studies should be carried out on the regeneration of MIL-53(Al) in continuous fixed-bed columns. Finally, more attention should be drawn on the adsorption mechanisms involved in using MOFs for removal of dyes in order to understand the adsorption performance of MOFs, which in turn will accelerate the development of novel materials for removal, separation, and adsorption.

References

- [1] S. Rodríguez-Couto, J. F. Osma and J. L. Toca-Herrera, "Removal of synthetic dyes by an eco-friendly strategy," *Engineering in Life Sciences*, vol. 9, no. 2, pp. 116-132, 2009.
- [2] M. Solís, A. Solís, H. I. Pérez, N. Manjarrez and M. Flores, "Microbial decolouration of azo dyes: A review," *Process Biochemistry*, vol. 47, no. 12, pp. 1723-1748, 2012.
- [3] V. Katheresan, J. Kansedo and S. Y. Lau, "Efficiency of various recent wastewater dye removal methods: A review," *Journal of Environmental Chemical Engineering*, vol. 6, no. 4, pp. 4676-4697, 2018.
- [4] "System Non-potable Water," Mechanical Contracting Education & Research Foundation (MCERF) , 2019. [Online]. Available: <http://opus.mcerf.org/application.aspx?id=-6228344935996635278>. [Accessed 5 October 2018].
- [5] P. Kumara, V. Bansalb, K.-H. Kimc and E. E. Kwond, "Metal-organic frameworks (MOFs) as futuristic options for wastewater treatment," *Journal of Industrial and Engineering Chemistry*, vol. 62, pp. 130-145, 2018.
- [6] J.-Q. Jiang, "The role of coagulation in water treatment," *Current Opinion in Chemical Engineering*, vol. 8, pp. 36-44, 2015.
- [7] W. Eckenfelder, D. L. Ford and A. J. Englande, *Industrial Water Quality*, New York: McGraw-Hill, 2009, pp. 60-67.
- [8] "Sewage Water Treatment Explained," Water Technology Engineering Ltd., 2019. [Online]. Available: http://www.crystaltanks.com/sewage_treatment_explained.html. [Accessed 20 October 2018].
- [9] M. T.Yagub, T. K. Sen, S. Afroze and H. Ang, "Dye and its removal from aqueous solution by adsorption: A review," *Advances in Colloid and Interface Science*, vol. 209, no. Supplement C, pp. 172-184, 2014.
- [10] G. Zeng, Z. Ye, Y. He, X. Yang, J. Ma, H. Shi and Z. Feng, "Application of dopamine-modified halloysite nanotubes/PVDF blend membranes for direct dyes removal from wastewater," *Chemical Engineering Journal*, vol. 232, pp. 572-583, 2017.
- [11] R. Kant, "Textile dyeing industry an environmental hazard," *Natural Science*, vol. 4, no. 1, pp. 22-26, 2012.
- [12] F. Gholami-Borujeni, A. Mahvi, S. Naseri, M. Faramarzi, R. Nabizadeh and M. Alimohmmadi, "Application of immobilized horseradish peroxidase for removal and detoxification of azo dye from aqueous solution," *Research Journal of Chemistry and Environment*, vol. 15, no. 2, pp. 217-222, 2011.
- [13] M. A. M. Salleh, D. K. Mahmoud, W. A. W. A. Karima and A. Idris, "Cationic and anionic dye adsorption by agricultural solid wastes: A comprehensive review," *Desalination*, vol. 280, no. 1-3, pp. 1-13, 2011.

- [14] V. Gupta and Suhas, "Application of low-cost adsorbents for dye removal – A review," *Journal of Environmental Management*, vol. 90, no. 8, p. 2313–2342, 2009.
- [15] G. R. Chatwal and M. Arora, *Synthetic Dyes*, Global Media, 2008.
- [16] N. P. Raval, P. U. Shah and N. K. Shah, "Nanoparticles Loaded Biopolymer as Effective Adsorbent for Adsorptive Removal of Malachite Green from Aqueous Solution," *Water Conservation Science and Engineering*, vol. 1, no. 1, pp. 69-81, 2016.
- [17] M. K. Uddin and U. Baig, "Synthesis of Co₃O₄ nanoparticles and their performance towards methyl orange dye removal: Characterisation, adsorption and response surface methodology," *Journal of Cleaner Production*, vol. 211, no. 1, pp. 1141-1153, 2019.
- [18] F. Bouaz, M. Kouba, F. Kallel, R. E. Ghorbel and S. E. Chaabouni, "Adsorptive removal of malachite green from aqueous solutions by almond gum: Kinetic study and equilibrium isotherms," *International Journal of Biological Macromolecules*, vol. 105, no. 1, pp. 56-65, 2017.
- [19] R. Gong, J. Ye, W. Dai, X. Yan, J. Hu, X. Hu, S. Li and H. Huang, "Adsorptive Removal of Methyl Orange and Methylene Blue from Aqueous Solution with Finger-Citron-Residue-Based Activated Carbon," *Industrial & Engineering Chemistry Research* 2013, vol. 52, no. 39, p. 14297–14303, 2013.
- [20] C. Grégorio, "Non-conventional low-cost adsorbents for dye removal: A review," *Bioresource Technology*, vol. 97, no. 9, pp. 1061-1085, 2006.
- [21] M. Sarro, N. P. Gule, E. Laurenti, R. Gamberini, M. C. Paganini, P. E. Mallon and P. Calza, "ZnO-based materials and enzymes hybrid systems as highly efficient catalysts for recalcitrant pollutants abatement," *Chemical Engineering Journal*, vol. 334, pp. 2530-2538, 2018.
- [22] M. A. M. Al-Alwani, N. A. Ludin, A. B. Mohamad, A. A. H. Kadhum and A. Mukhlus, "Application of dyes extracted from *Alternanthera dentata* leaves and *Musa acuminata* bracts as natural sensitizers for dye-sensitized solar cells," *Spectrochimica Acta Part A: Molecular and Biomolecular Spectroscopy*, vol. 192, pp. 487-498, 2018.
- [23] T. Robinson, G. McMullan, R. Marchant and P. Nigam, "Remediation of dyes in textile effluent: a critical review on current treatment technologies with a proposed alternative," *Bioresource Technology*, vol. 77, no. 3, pp. 247-255, 2001.
- [24] Y. Pan, Y. Wang, A. Zhou, A. Wang, Z. Wu, L. Lv, X. Li, K. Zhang and T. Zhu, "Removal of azo dye in an up-flow membrane-less bioelectrochemical system integrated with bio-contact oxidation reactor," *Chemical Engineering Journal*, vol. 326, pp. 454-461, 2017.
- [25] K. A. Adegoke and O. S. Bello, "Dye sequestration using agricultural wastes as adsorbents," *Water Resources and Industry*, vol. 12, pp. 8-24, 2015.
- [26] A. Srinivasan and T. Viraraghavan, "Decolorization of dye wastewaters by biosorbents: A review," *Journal of Environmental Management*, vol. 91, no. 10, pp. 1915-1929, 2010.

- [27] Y. Slokar and A. L. Marechal, "Methods of decoloration of textile wastewaters," *Dyes and Pigments*, vol. 37, no. 4, pp. 335-356, 1998.
- [28] D. Pak and W. Chang, "Decolorizing dye wastewater with low temperature catalytic oxidation," *Water Science and Technology*, vol. 30, no. 4-5, pp. 115-121, 1999.
- [29] Y. Xu, R. Lebrun, P.-J. Gallo and P. Blond, "Treatment of textile dye plant effluent by nanofiltration membrane," *Separation Science and Technology*, vol. 34, no. 13, pp. 2501-2519, 1999.
- [30] P. Peralto-Zamora, A. Kunz, S. G. d. Morales, R. Pelegrini, P. d. C. Moleiro, J. Reyes and N. Duran, "Degradation of reactive dyes I. A comparative study of ozonation, enzymatic and photochemical processes," *Chemosphere*, vol. 38, pp. 835-852, 1999.
- [31] Y. Yang, D. W. II and M. Bahorsky, "Decolorization of dyes using UV/H₂O₂ photochemical oxidation," *Textile Chemist and Colorist*, vol. 30, no. 4, pp. 27-35, 1998.
- [32] R. Pelegrini, P. Peralto-Zamora, A. d. Andrade, J. Reyers and N. Duran, "Electrochemically assisted photocatalytic degradation of reactive dyes," *Pelegrini, R.; Peralta-Zamora, P.; De Andrade, A.R.; Reyes, J.; Durán, N.*, vol. 22, no. 2, pp. 83-90, 1999.
- [33] "Membrane Filtration," November 2005. [Online]. Available: <https://www.mrwa.com/WaterWorksMnl/Chapter%2019%20Membrane%20Filtration.pdf>. [Accessed 1 November 2018].
- [34] Mohd.Rafatullah, O. Sulaiman, R. Hashim and A. Ahmad, "Adsorption of methylene blue on low-cost adsorbents: A review," *Journal of Hazardous Materials*, vol. 177, no. 1-3, pp. 70-80, 2010.
- [35] A. Dąbrowski, "Adsorption — from theory to practice," *Advances in Colloid and Interface Science*, vol. 93, no. 1-3, pp. 135-224, 2001.
- [36] A. Ahmad, S. H. Mohd-Setapar, C. S. Chuong, A. Khatoon, W. A. Wani, R. Kumard and M. Rafatullah, "Recent advances in new generation dye removal technologies: novel search for approaches to reprocess wastewater," *RSC Advances*, vol. 5, no. 39, pp. 30801-30818, 2015.
- [37] N. Ballav, R. Das, S. Giri, A. M.Muliwa, K. Pillay and A. Maity, "l-cysteine doped polypyrrole (PPy@L-Cyst): A super adsorbent for the rapid removal of Hg⁺² and efficient catalytic activity of the spent adsorbent for reuse," *Chemical Engineering Journal*, vol. 345, pp. 621-630, 2018.
- [38] S. D. Gisi, G. Lofrano, M. Grassi and M. Notarnicola, "Characteristics and adsorption capacities of low-cost sorbents for wastewater treatment: A review," *Sustainable Materials and Technologies*, vol. 9, pp. 10-40, 2016.
- [39] I. Bouzaida and M. Rammah, "Adsorption of acid dyes on treated cotton in a continuous system," *Materials Science and Engineering: C*, vol. 21, no. 1-2, pp. 151-155, 2002.

- [40] S. Montoya-Suarez, F. Colpas-Castillo, E. Meza-Fuentes, J. Rodríguez-Ruiz and R. Fernandez-Maestre, "Activated carbons from waste of oil-palm kernel shells, sawdust and tannery leather scraps and application to chromium(VI), phenol, and methylene blue dye adsorption," *Water Science & Technology*, vol. 73, no. 1, pp. 21-27, 2015.
- [41] Y. Peng, Y. Zhang, H. Huang and C. Zhong, "Flexibility induced high-performance MOF-based adsorbent for nitroimidazole antibiotics capture," *Chemical Engineering Journal*, vol. 333, pp. 678-685, 2018.
- [42] N. A. Khan, B. NathBhadra and S. HwaJhung, "Heteropoly acid-loaded ionic liquid@metal-organic frameworks: Effective and reusable adsorbents for the desulfurization of a liquid model fuel," *Chemical Engineering Journal*, vol. 334, pp. 2215-2221, 2018.
- [43] Q. Zhao, F. Wu, K. Xie, R. Singh, J. Zhao, P. Xiao and P. A. Webley, "Synthesis of a novel hybrid adsorbent which combines activated carbon and zeolite NaUSY for CO₂ capture by electric swing adsorption (ESA)," *Chemical Engineering Journal*, vol. 336, pp. 659-668, 2018.
- [44] L. Tang, J. Yu, Y. Pang, G. Zeng, Y. Deng, J. Wang, X. Ren, S. Ye, B. Peng and H. Feng, "Sustainable efficient adsorbent: Alkali-acid modified magnetic biochar derived from sewage sludge for aqueous organic contaminant removal," *Chemical Engineering Journal*, vol. 336, pp. 160-169, 2018.
- [45] C. Woolard, J. Strong and C. Erasmus, "Evaluation of the use of modified coal ash as a potential sorbent for organic waste streams," *Applied Geochemistry*, vol. 17, no. 8, pp. 1159-1164, 2002.
- [46] "What is Zeolite," Rota mining corporation, [Online]. Available: <http://www.rotamining.com/what-is-zeolite/>. [Accessed 5 November 2018].
- [47] S. Kitagawa, R. Kitaura and S. Noro, "Functional Porous Coordination Polymers," *Angewandte Chemie*, vol. 43, no. 18, pp. 2334-2375, 2004.
- [48] K. A. Cychosz, A. G. Wong-Foy and A. J. Matzger, "Liquid Phase Adsorption by Microporous Coordination Polymers: Removal of Organosulfur Compounds," *Journal of the american chemical society*, vol. 130, no. 22, p. 6938-6939, 2008.
- [49] Y. Liu, V. C. Kravtsov, R. Larsen and M. Eddaoudi, "Molecular building blocks approach to the assembly of zeolite-like metal-organic frameworks (ZMOFs) with extra-large cavities," *Chemical Communications*, vol. 14, pp. 1488-1490, 2006.
- [50] S. Ma and H.-C. Zhou, "A Metal-Organic Framework with Entatic Metal Centers Exhibiting High Gas Adsorption Affinity," *Journal of the american chemical society*, vol. 128, no. 36, pp. 11734-11735, 2006.
- [51] S. H. J. Zubair Hasan, "Removal of hazardous organics from water using metal-organic frameworks (MOFs): Plausible mechanisms for selective adsorptions," *Journal of Hazardous Materials*, vol. 283, pp. 329-339, 2015.
- [52] A. C. Tella and I. Y. Aaron, "Syntheses and applications of metal-organic frameworks materials: a review," *Acta chimica & Pharmaceutica Indica*, vol. 2, no. 2, pp. 75-81, 2012.

- [53] N. A. Khan and S. H. Jung, "Adsorptive removal and separation of chemicals with metal-organic frameworks: contribution of pi-complexation," *Journal of Hazardous Materials*, vol. 325, p. 198–213, 2017.
- [54] J.-R. Li, J. Sculley and H.-C. Zhou, "Metal-organic frameworks for separations," *Chemical Reviews*, vol. 112, pp. 869-932, 2012.
- [55] G. Férey, "Hybrid porous solids: past, present, future," *Chemical Society Reviews*, vol. 37, no. 1, pp. 191-214, 2008.
- [56] J. Juan-Alcañiz, R. Gielisse, A. Lago, E. Ramos-Fernandez, P. Serra-Crespo, T. Devic, N. Guillou, C. Serre, F. Kapteijn and J. Gascon, "Towards acid MOFs-catalytic performance of sulfonic acid functionalized architectures," *Catalysis Science and Technology*, vol. 3, no. 9, pp. 2311-2318, 2013.
- [57] Y. Hwang, D.-Y. Hong, J.-S. Chang, S. Jung, Y.-K. Seo, J. Kim, A. Vimont, M. Daturi, C. Serre and G. Férey, "Amine grafting on coordinatively unsaturated metal centers of MOFs: consequences for catalysis and metal encapsulation," *Angewandte Chemie - International Edition*, vol. 47, no. 22, pp. 4144-4148, 2008.
- [58] J. Cavka, S. Jakobsen, U. Olsbye, N. Guillou, C. Lamberti, S. Bordiga and K. Lillerud, "A new zirconium inorganic building brick forming metal organic frameworks with exceptional stability," *J.H. Cavka, S. Jakobsen, U. Olsbye, N. Guillou, C. Lamberti, S. Bordiga, K.P. Lillerud*, vol. 130, no. 42, pp. 13850-13851, 2008.
- [59] D. Britt, C. Lee, F. Uribe-Romo, H. Furukawa and O. Yaghi, "Ring-opening reactions within porous metal-organic frameworks," *Inorganic Chemistry*, vol. 49, no. 14, pp. 6387-6389, 2010.
- [60] M. Goestena, J. Juan-Alcañiz, E. Ramos-Fernandez, K. Gupta, E. Stavitski, H. Bekkum, J. Gascon and F. Kapteijn, "Sulfation of metal-organic frameworks: opportunities for acid catalysis and proton conductivity," *Journal of Catalysis*, vol. 281, p. 177, 2011.
- [61] J. Canivet, A. Fateeva, Y. Guo, B. Coasne and D. Farrusseng, "Water adsorption in MOFs: fundamentals and applications," *Chemical Society Reviews*, vol. 43, no. 16, pp. 5594-5617, 2014.
- [62] B. Valizadeh, T. N. Nguyen and K. C. Stylianou, "Shape engineering of metal-organic frameworks," *Polyhedron*, vol. 145, pp. 1-15, 2018.
- [63] N. A. Khan, Z. Hasan and S. H. Jung, "Adsorptive removal of hazardous materials using metal-organic frameworks (MOFs): A review," *Journal of Hazardous Materials*, Vols. 244-245, pp. 444-456, 2013.
- [64] E. Haque, J. E. Lee, I. T. Jang, Y. K. Hwang, J.-S. Chang, J. Jegal and S. H. Jung, "Adsorptive removal of methyl orange from aqueous solution with metal-organic frameworks, porous chromium-benzenedicarboxylates," *Journal of Hazardous Materials*, vol. 181, no. 1-3, pp. 535-542, 2010.
- [65] A. Ayati, M. N. Shahrak, B. Tanhaei and M. Sillanpaa, "Emerging adsorptive removal of azo dye by metaleorganic," *Chemosphere*, vol. 160, pp. 30-44, 2016.

- [66] K.-Y. A. Lin and H.-A. Chang, "Ultra-high adsorption capacity of zeolitic imidazole framework-67 (ZIF-67) for removal of malachite green from water," *Chemosphere*, vol. 139, pp. 624-631, 2015.
- [67] A. K. Ebrahimi, I. Sheikshoaie and M. Mehran, "Facile synthesis of a new metal-organic framework of copper (II) by interface reaction method, characterization, and its application for removal of Malachite Green," *Journal of Molecular Liquids*, vol. 240, pp. 803-809, 2017.
- [68] Z. Shi, C. Xu, H. Guan, L. Li, L. Fan, Y. Wang, L. Liu, Q. Meng and R. Zhang, "Magnetic metal organic frameworks (MOFs) composite for removal of lead and malachite green in wastewater," *Colloids and Surfaces A*, vol. 539, pp. 382-390, 2018.
- [69] S. Dhaka, R. Kumar, A. Deep, M. B. Kurade, S.-W. Ji and B.-H. Jeon, "Metal-organic frameworks (MOFs) for the removal of emerging contaminants from aquatic environments," *Coordination Chemistry Reviews*, vol. 380, no. 1, pp. 330-352, 2019.
- [70] C. Li, Z. Xiong, J. Zhang and C. Wu, "The Strengthening Role of the Amino Group in Metal-Organic Framework MIL-53 (Al) for Methylene Blue and Malachite Green Dye Adsorption," *Journal of Chemical & Engineering Data*, vol. 60, no. 11, pp. 3414-3422, 2015.
- [71] X.-P. Luo, S.-Y. Fu, Y.-M. Du, J.-Z. Guo and B. Li, "Adsorption of methylene blue and malachite green from aqueous solution by sulfonic acid group modified MIL-101," *Microporous and Mesoporous Materials*, vol. 237, no. 1, pp. 268-274, 2017.
- [72] H. Liu, L. Chen and J. Ding, "Adsorption behavior of magnetic amino-functionalized metal-organic framework for cationic and anionic dyes from aqueous solution," *RSC Advances*, vol. 6, no. 54, pp. 48884-48895, 2016.
- [73] E. Haque, J. W. Jun and S. H. Jung, "Adsorptive removal of methyl orange and methylene blue from aqueous solution with a metal-organic framework material, iron terephthalate (MOF-235)," *Journal of Hazardous Materials*, vol. 185, no. 1, pp. 507-511, 2011.
- [74] S.-c. Wu, X. You, C. Yang and J.-h. Cheng, "Adsorption behavior of methyl orange onto an aluminum-based metal organic framework, MIL-68(Al)," *Water Science & Technology*, vol. 75, no. 12, pp. 2800-2810, 2017.
- [75] M. Tong, D. Liu, Q. Yang, S. Devautour-Vinot, G. Maurin and C. Zhong, "Influence of framework metal ions on the dye capture behavior of MIL-100 (Fe, Cr) MOF type solids," *Journal of Materials Chemistry A*, vol. 1, no. 30, p. 8534, 2013.
- [76] E. Haque, V. Lo, A. I. Minett, A. T. Harrisa and T. L. Church, "Dichotomous adsorption behaviour of dyes on an amino-functionalised metal-organic framework, amino-MIL-101(Al)," *Journal of Materials Chemistry A*, vol. 2, no. 1, p. 193-203, 2014.
- [77] X. Qian, B. Yadian, R. Wu, Y. Long, K. Zhou, B. Zhu and Y. Huang, "Structure stability of metal-organic framework MIL-53 (Al) in aqueous solutions," *International Journal of Hydrogen Energy*, vol. 38, no. 36, pp. 16710-16715, 2013.

- [78] Y. Wu, M. Su, J. Chen, Z. Xu, J. Tang, X. Chang and D. Chen, "Superior adsorption of methyl orange by h-MoS₂ microspheres: Isotherm, kinetics, and thermodynamic studies," *Dyes and Pigments*, vol. 170, p. 107591, 2019.
- [79] S. Milonjić, A. Ruvarac and M. Šušić, "The heat of immersion of natural magnetite in aqueous solutions," *Thermochimica Acta*, vol. 11, no. 3, pp. 261-266, 1975.
- [80] Y. S. Ho and G. McKay, "Pseudo-second order model for sorption process," *Process Biochem*, vol. 34, pp. 451-465, 1999.
- [81] T. K.L. and B. Hameed, "Insight into the adsorption kinetics models for the removal of contaminants from aqueous solutions," *Journal of the Taiwan Institute of Chemical Engineers*, vol. 74, pp. 25-48, 2017.
- [82] M. K. Dahri, M. R. R. Kooch and L. B. Lim, "Application of Casuarina equisetifolia needle for the removal of methylene blue and malachite green dyes from aqueous solution," *Alexandria Engineering Journal*, vol. 54, no. 1, pp. 1253-1263, 2015.
- [83] M. Özacara and A. Şengil, "Application of kinetic models to the sorption of disperse dyes onto alunite," *Colloids and Surfaces A: Physicochemical and Engineering Aspects*, vol. 242, no. 1-3, pp. 105-113, 2004.
- [84] M. T. Yagub, T. K. Sen, S. Afroze and H. Ang, "Dye and its removal from aqueous solution by adsorption: A review," *Advances in Colloid and Interface Science*, vol. 209, pp. 172-184, 2014.
- [85] L. Xiao, Y. Xiong, S. Tian, C. He, Q. Su and Z. Wen, "One-dimensional coordination supramolecular polymer [Cu(bipy)(SO₄)]_n as an adsorbent for adsorption and kinetic separation of anionic dyes," *Chemical Engineering Journal*, vol. 265, p. 157-163, 2015.
- [86] X.-j. Hu, J.-s. Wang, Y.-g. Liu, X. Li, G.-m. Zeng, Z.-l. Bao, X.-x. Zeng, A.-w. Chen and F. Long, "Adsorption of chromium (VI) by ethylenediamine-modified cross-linked magnetic chitosan resin: Isotherms, kinetics and thermodynamics," *Journal of Hazardous Materials*, vol. 185, no. 1, pp. 306-314, 2011.
- [87] K. Chai, K. Lu, Z. Xu, Z. Tong and H. Ji, "Rapid and selective recovery of acetophenone from petrochemical effluents," *Journal of Hazardous Materials*, vol. 348, no. 1, pp. 20-28, 2018.
- [88] F. Geyikçi and H. Büyükgüngör, "Factorial experimental design for adsorption silver ions from water onto Montmorillonite," *Acta Geodynamica et Geomaterialia*, vol. 10, no. 3, pp. 363-370, 2013.
- [89] M. Carmona, M. d. Silva and S. Leite, "Biosorption of chromium using factorial experimental design," *Process Biochemistry*, vol. 40, no. 2, pp. 779-788, 2005.
- [90] J. Brasil, R. Ev, C. Milcharek, L. Martins, F. Pavan, A. d. S. Jr, S. Dias, J. Dupont, C. Noreña and E. Lima, "Statistical design of experiments as a tool for optimizing the batch conditions to Cr (VI) biosorption on Araucaria angustifolia wastes," *Journal of Hazardous Materials*, vol. 133, no. 1-3, pp. 143-153, 2006.

- [91] M. A. Aly-Eldeen, A. A. El-Sayed, D. M. Salem and G. M. Zokm, "The uptake of Eriochrome Black T dye from aqueous solutions utilizing waste activated sludge: Adsorption process optimization using factorial design," *The Egyptian Journal of Aquatic Research*, vol. 44, no. 3, pp. 179-186, 2018.
- [92] V. I. Isaeva, O. L. Eliseev, R. V. Kazantsev, V. V. Chernyshev, A. L. Tarasov, P. E. Davydov, A. L. Lapidus and L. M. Kustov, "Effect of the support morphology on the performance of Co nanoparticles deposited on metal-organic framework MIL-53(Al) in Fischer-Tropsch synthesis," *Polyhedron*, vol. 157, pp. 389-395, 2019.
- [93] M. Zhou, Y.-N. Wu, J. Qiao, J. Zhang, A. McDonald, G. Li and F. Li, "The removal of bisphenol A from aqueous solutions by MIL-53(Al) and mesostructured MIL-53(Al)," *Journal of Colloid and Interface Science*, vol. 405, pp. 157-163, 2013.
- [94] Y. Guan, M. Xia, X. Wang, W. Cao and A. Marchetti, "Water-based preparation of nano-sized NH₂-MIL-53(Al) frameworks for enhanced dye removal," *Inorganica Chimica Acta*, vol. 484, pp. 180-184, 2019.
- [95] K. Mahmoudi, N. Hamdi, A. Kriaa and E. Srasra, "Adsorption of methyl orange using activated carbon prepared from lignin by ZnCl₂ treatment," *Russian Journal of Physical Chemistry A*, vol. 86, no. 8, p. 1294-1300, 2012.
- [96] B. Hameed, "Grass waste: a novel sorbent for the removal of basic dye from aqueous solution," *Journal of Hazardous Materials*, vol. 166, no. 1, pp. 233-238, 2009.
- [97] D. Ding, Z. Zhang, R. Chen and T. Cai, "Selective removal of cesium by ammonium molybdophosphate – polyacrylonitrile bead and membrane," *Journal of Hazardous Materials*, vol. 324, no. 1, pp. 753-761, 2017.
- [98] X. Sun, L. Yang, Q. Li, Z. Liu, T. Dong and H. Liu, "Polyethylenimine-functionalized poly(vinyl alcohol) magnetic microspheres as a novel adsorbent for rapid removal of Cr(VI) from aqueous solution," *Chemical Engineering Journal*, vol. 262, no. 1, pp. 101-108, 2015.
- [99] W. Ruixia, C. Jinlong, C. Lianlong, F. Zheng-hao, L. Ai-min and Z. Quanxing, "Study of adsorption of lipoic acid on three types of resin," *Reactive and Functional Polymers*, vol. 59, no. 3, pp. 243-252, 2004.
- [100] A. Regti, A. E. Kassimi, M. R. Laamari and M. E. Haddad, "Competitive adsorption and optimization of binary mixture of textile dyes: A factorial design analysis," *Journal of the Association of Arab Universities for Basic and Applied Sciences*, vol. 24, no. 1, pp. 1-9, 2017.
- [101] A. M. Ghaedi, M. Panahimehr, A. R. S. Nejad, S. J. Hosseini, A. Vafaei and M. M. Baneshi, "Factorial experimental design for the optimization of highly selective adsorption removal of lead and copper ions using metal organic framework MOF-2 (Cd)," *Journal of Molecular Liquids*, vol. 272, no. 1, pp. 15-26, 2018.

Vita

Miral Al Sharabati was born in 1995, in Abu Dhabi, United Arab Emirates. She received her primary and secondary education from Rosary School in Abu Dhabi, UAE. She received her B.Sc. degree in Chemical Engineering from Abu Dhabi University in 2017. From 2017 to 2018, she worked as a water treatment sales engineer in Concorde-Corodex Group.

In January 2018, she joined the Chemical Engineering master's program in the American University of Sharjah. She was awarded the Graduate Teaching Assistantship till 2019. Her research interests are in water and waste-water treatment as well as the different applications of Metal Organic Frameworks in sustainable energy technologies.